# Analyzing and Tuning the Chalcogen-Amine-Thiol Complexes for Tailoring of Chalcogenide Syntheses

Swapnil D. Deshmukh,<sup>†</sup> Leah F. Easterling,<sup>‡</sup> Jeremy M. Manheim,<sup>‡</sup> Nicole J. LiBretto,<sup>†</sup> Kyle G. Weideman,<sup>†</sup> Jeffrey T. Miller,<sup>†</sup> Hilkka I. Kenttämaa,<sup>‡</sup> and Rakesh Agrawal<sup>†</sup>\*

<sup>†</sup>Davidson School of Chemical Engineering, Purdue University, 480 Stadium Mall Drive, West Lafayette, IN 47907, United States

<sup>‡</sup>Department of Chemistry, Purdue University, 560 Oval Drive, West Lafayette, Indiana 47907, United States

### **Abstract:**

The amine-thiol solvent system has been used extensively to synthesize metal chalcogenide thin films and nanoparticles due to its ability to dissolve various metal and chalcogen precursors. While previous studies of this solvent system have focused on understanding the dissolution of metal precursors, here we provide an in-depth investigation of the dissolution of chalcogens, specifically Se and Te. Analytical techniques including Raman, X-ray absorption, NMR spectroscopy, and high-resolution tandem mass spectrometry were used to identify pathways for Se and Te dissolution in butylamine-ethanethiol and ethylenediamine-ethanethiol solutions. Se in monoamine-monothiol solutions was found to form ionic polyselenides free of thiol ligands while in diamine-monothiol solutions thiol coordination with polyselenides was predominately observed. By increasing the relative concentration of thiol to that of Se, the chain length of polyselenide species was observed to shorten. Analysis of Te dissolution in diamine-thiol solutions also suggested the formation of relatively unstable thiol-coordinated Te ions. This instability of Te ions was found to be reduced by co-dissolving Te with Se in diamine-thiol solutions. Analysis of the co-dissolved solutions revealed the presence of atomic interaction between Se and Te through the identification of Se-Te bonds. This new understanding then provided a new route to dissolve otherwise insoluble Te in butylamine-ethanethiol solution by taking advantage of the Se<sup>2-</sup> nucleophile. Finally, the knowledge gained for chalcogen dissolutions in this solvent system allowed for controlled alloying of Se and Te in PbSe<sub>n</sub>Te<sub>1-n</sub> material and also provided a general knob to alter various metal chalcogenide material syntheses.

### **Introduction:**

Metal chalcogenide materials have significant applications in the field of semiconductors, including photovoltaics, thermoelectric devices, LED's, and sensors, amongst others.<sup>1,2</sup> Traditional fabrication routes for these devices include processes such as co-evaporation and cosputtering, which are expensive and energy intensive as they require processing under very low pressure (high vacuum) atmosphere. Solution processing, with its mild processing conditions, improved material utilization, ability to make thin films using roll to roll processing, and low energy requirements, is a promising and less expensive alternative fabrication route. 3-5 Recent developments in solution processing provide two methods for material synthesis and device fabrication. The first route involves synthesis of the desired material in the form of nanoparticles followed by dispersing the nanoparticles in organic/aqueous solvents for ink formulation. The second route is direct deposition of a molecular precursor solution followed by thermal annealing to yield the desired material in thin film architecture.

Although solution processing is a promising cost effective alternative to vacuum processing, developing a common solvent system to dissolve various material precursors has been a challenge. Various organic solvents, including but not limited to DMSO, DMF, and alcohols, have been used to incorporate metal salt precursors and successfully fabricate metal sulfide materials.<sup>6,7</sup> Despite these successes, fabricating metal selenide and telluride materials has been challenging due to the difficulties involved in dissolution of Se and Te in these solvents. Several other solvent systems have been explored to dissolve Se and Te, but most of these systems either require highly toxic and explosive chemicals like hydrazine or introduce impurities into the final material (e.g., alkyl phosphine or borohydride systems).<sup>8-11</sup> Recently, aminethiol solvent system have shown great promise in dissolving a variety of precursors, including metals, metal salts, metal chalcogenides and even pure chalcogens like S. Se and Te at ambient conditions and in considerably high concentrations. 12-16 Researchers have utilized this new solvent system for fabricating a variety of chalcogenide

including  $(Cu,Ag)(In,Ga)(S,Se)_2$ , materials. (Cu,Ag)<sub>2</sub>ZnSn(S,Se)<sub>4</sub>, CdTe, CuBaSnS<sub>4</sub>, SnTe, Sb<sub>2</sub>Se<sub>3</sub>. PbS/Se/Te, etc. in the form of thin films as well as nanoparticles for applications in photovoltaic and thermoelectric devices. 13-23 Although successful material fabrication has been achieved using amine-thiol solvent system, few studies have highlighted the complexity of the products formed when using these solutions. For example, recent studies on amine-thiol solution used to dissolve CuCl<sub>2</sub>/CuCl and Cu precursors identified the formation of numerous complex products, which could impact the film fabrication process.<sup>24,25</sup> Therefore, realizing the full potential of amine-thiol solvent system requires a better understanding of the underlying chemistry involved in their dissolution mechanisms.

In the case of chalcogens, Walker and Agrawal reported Se removal from reaction mixture of metal selenide particles synthesized in oleylamine by addition of hexanethiol in the solution.<sup>26</sup> During similar period, Liu et al. reported dissolution of Se in oleylamine and dodecanethiol solution for the synthesis of Cu(In,Ga)Se<sub>2</sub>, Cu<sub>2</sub>ZnSnSe<sub>4</sub>, and CdSe nanoparticles.<sup>27</sup> This was followed by a report from Brutchey's group on Se and Te dissolution in an ethylenediamine-ethanethiol system. The study demonstrated impurity-free recovery of elemental Se and Te through solvent evaporation and also used these solutions to synthesize crystalline Sb<sub>2</sub>Se<sub>3</sub> and SnTe materials.<sup>15</sup> Similarly, an array of amine-ethanethiol systems were used by Walker and Agrawal for the dissolution of Se and was further modified to create a sulfur-free selenium precursor for the synthesis of Se, PbSe, CuInSe<sub>2</sub> and Cu<sub>2</sub>ZnSnSe<sub>4</sub> nanoparticles. <sup>16</sup> While these solutions have been utilized for material synthesis, very little research has been conducted to analyze the solutions themselves. For example, it is known that Te dissolves only in amine-thiol systems made with diamines while Se dissolves in amine-thiol systems made from both diamines and monoamines: however, the dissolution mechanism(s) and speciation in these solutions mostly remains unexplored.

In this work, we have analyzed chalcogen dissolution in amine-thiol solutions by using various analytical techniques, including Raman spectroscopy, <sup>1</sup>H-NMR spectroscopy, electrospray ionization high-resolution tandem mass spectrometry, and X-ray absorption spectroscopy. We have identified the differences between the species formed when Se is dissolved in monoamine-monothiol solutions versus diamine-monothiol solutions. Additionally, we have studied the relationship between the mol ratio of thiol:Se used in the dissolution with the corresponding Se species formed. This analysis provided key information that adds to the current understanding of Se dissolution in amine-thiol solutions. As Te dissolves only in diamine-thiol solutions, we analyzed Te dissolution

in diamine-monothiol systems and found some similarities and some differences to the corresponding Se solutions. We further extended this new understanding of Se and Te dissolution to study the co-dissolution of these two chalcogens in amine-thiol solutions, which revealed an atomic interaction between Se and Te complexes. This observed interaction between Se and Te in the solution provided the foundation for the development of a new dissolution pathway for incorporating Te in monoaminemonothiol solutions. The Se-Te complex was then utilized to synthesize a PbSe<sub>n</sub>Te<sub>1-n</sub> alloy that demonstrated a controlled extent of chalcogen alloying based on the Se-Te solution used in the synthesis. Our findings from this work can further be used to provide preliminary reasoning for the differences observed when chalcogenide materials are synthesized using different amine-thiol solvent pairs.

# **Experimental Section:**

### **Materials**

Se (100 mesh, 99.99%), Te (30 mesh, 99.997%), butylamine (BA, 99.5%), ethylenediamine (EN, >99.5%), diethyl disulfide (DEDS, 99%) and lead acetate trihydrate (99.999%) were purchased from Sigma-Aldrich while ethanethiol (ET, 99%) was purchased from Acros Organics. All chemicals were used without further purification.

### **Ink Formulation and Reaction**

Various inks for Se and Te solutions were prepared by adding either butylamine (BA) or ethylenediamine (EN) to the Se or Te powder followed by the addition of ethanethiol (ET). Se solutions containing significant amounts of thiol were completely dissolved within a few minutes of solvent addition while Se solutions with lesser quantities of thiol and all Te solutions were stirred for several hours to obtain complete dissolution. All solid weighing and solution preparation were performed in an inert nitrogen atmosphere in a glovebox (oxygen and moisture concentrations less than 1 ppm). Since ET boils at 35 °C, vials were further sealed with parafilm to avoid loss of ET from the vials due to evaporation.

For PbSe<sub>n</sub>Te<sub>1-n</sub> material synthesis, a 0.2 M solution of lead acetate trihydrate was prepared in pure EN solvent. Chalcogen solutions were prepared by co-dissolving Se and Te in both BA-ET and EN-ET solutions (amine/thiol volume ratio of 1). Se:Te mol ratio of 4:1 was used in both the dissolutions while keeping total chalcogen concentration (Se+Te) at 0.2 M. 1 ml of lead acetate solution was mixed with 1 ml of chalcogen solution under constant stirring for 1 min at room temperature. Particles formed via immediate precipitation were centrifuged and then washed once with EN in the glovebox followed by

three isopropyl alcohol washes in air to remove the excess amine-thiol solution from the reaction mixture.

### Characterization

**Raman Spectroscopy:** Raman spectra were collected on a Horiba/Jobin-Yvon HR800 microscope with an excitation laser wavelength of 632.8 nm and resolution of 0.3 cm<sup>-1</sup> at 1800 grating. Liquid samples were sealed in a Hellma Analytics fluorescence quartz cuvette in a glove box prior to analysis. The laser power was adjusted to 4.25 mW for analysis of all samples.

**Nuclear Magnetic Resonance:** NMR spectra were collected using a Brucker AV-III-400-HD instrument. Deuterated acetonitrile was used as a solvent for this analysis. For quantitative measurements, ethylene carbonate was used as the NMR standard.

**X-ray Absorption Spectroscopy:** In situ X-ray absorption spectroscopy (XAS) experiments were performed at the 10-BM beamline at the Advanced Photon Source (APS) at Argonne National Laboratory. Measurements were performed at the Se K edge (12.6580 keV) and Te K edge (31.8138 keV) in transmission mode using a fast scan from 250 eV below the edge to 550 eV above the edge, which took approximately 10 minutes per scan. Se edge samples were prepared at 0.1 M Se concentration in solution while Te edge sample was prepared at 0.5 M Te concentration in solution. All samples were sealed in a liquid sample cell in an air-free atmosphere. Standard fitting procedures were used to fit the EXAFS. Intrinsic loss factor S<sub>0</sub><sup>2</sup> was calibrated by fitting the foil and was found to be 0.75. A least squared fit for the first shell of r- space and isolated qspace were performed on the k<sup>2</sup> weighted Fourier transform data over the range 2.7 to 10 Å<sup>-1</sup> in each spectrum to fit the magnitude and imaginary components. Se-Se (CN=1, R=2.35 Å), Se-Te (CN=1, R=2.52 Å), Se-S (CN=1, R=2.24 Å), Te-Te (CN=1, R=2.73 Å) and Te-S (CN=1, R=2.42 Å) scattering pairs were considered using FEFF6 calculations.<sup>28</sup> The error in the coordination number calculation is +/- 10 % and the error in the bond distance is +/- 0.01 Å.

*Electrospray Ionization High-Resolution Tandem Mass Spectrometry ((-)ESI-MS/MS):* The mass spectrometry experiments conducted for this study were based on previous work on copper dissolution in similar amine-thiol solutions. <sup>24</sup> To avoid air contact with the solutions during mass spectrometry measurements, the solutions were prepared in a glovebox and then transferred to a setup containing a 5 mL Hamilton syringe, 500 μL Hamilton syringe, and a high purity perfluoroalkoxy tubing, all connected via a three-way Hamilton valve. All experiments were conducted using a Thermo Scientific LTQ Orbitrap XL hybrid mass spectrometer, set to a resolution of

100,000. Ionization was accomplished using electrospray ionization (ESI). Solutions were directly infused into the ESI source by using a syringe pump at a flow rate of 10 μL/min. The spray voltage was adjusted daily to maintain an appropriate current for ionization and typical values ranged from 3 up to 4 kV. Sheath and auxiliary gases (N<sub>2</sub>) were set at 30 and 15 (arbitrary units) flow rates, respectively. The capillary temperature was maintained at 250 °C. The elemental composition for each component was determined from the high-resolution mass spectra as well as matching isotopic distribution patterns (when and confirmed using tandem appropriate) spectrometry based on collision-activated dissociation experiments (CAD). All CAD experiments were performed in the linear quadrupole ion trap with a q value of 0.25 and an activation time of 30 ms. The ion isolation window was adjusted for each ion so that only the ions of interest were isolated. Isolation windows ranged from  $\pm 0.4$ -1 m/z units. CAD energy was varied from 10-40 arbitrary units and was adjusted for each ion of interest to provide reliable fragmentation at sufficient signal intensity. All data processing was performed with the Thermo Scientific Xcalibur 2.1 software.

*Material characterization:* X-ray diffractograms (XRD) were obtained using a Rigaku Smart Lab diffractometer in Bragg–Brentano mode, using a Cu Kα ( $\lambda$  = 1.5406 Å) source operating at 40 kV/44 mA. Sample for XRD analysis was prepared by drop casting powder sample dispersed in isopropyl alcohol on a piece of soda lime glass. Bulk nanoparticle composition was analyzed using a Fisher XAN 250 X-ray fluorescence (XRF) instrument at 50 kV voltage with primary Ni filter containing silicon drift detector. Scanning electron microscopy (SEM) images were collected using FEI Quanta 3DSEM at an accelerating voltage of 10 kV, 4.0 spot size, and working distance of ~10 mm.

### **Result and Discussion:**

# **Selenium Dissolution in Monoamine vs Diamine Solutions:**

Selenium is known to dissolve in both monoamine-monothiol solutions and diamine-monothiol solutions at considerably high concentrations (Se  $\sim$  6 M and Te  $\sim$  0.6 M) at ambient conditions. <sup>15</sup> Previous analysis of these solutions revealed the formation of dialkyl disulfide species in monoamine-monothiol solutions but not in diamine-monothiol solutions suggesting a difference in Se species formed in the two solutions. <sup>15,16</sup> In order to understand the difference in Se dissolution in different amine-thiol solutions and hence the Se species formed in these systems, two separate 0.1 M Se solutions were prepared in this study:

one in 1:1 (v/v) butylamine-ethanethiol (BA-ET) and other in 1:1 (v/v) ethylenediamine-ethanethiol (EN-ET) such that the mol ratio of ET:Se in both these solutions is around 69. These two solutions were analyzed with various characterization techniques.

Raman analysis performed on the two solutions showed differences in Se bonding (Figure 1a). When compared to the pure BA-ET solutions, the Se in BA-ET solution revealed a presence of new peaks in the Raman spectrum with one relatively intense peak at 244 cm<sup>-1</sup> while another broad peak around 275 cm<sup>-1</sup>. Based on the literature, these new peaks correspond to Se-Se bonds. In solid state Se material, peaks in the vicinity of 234 cm<sup>-1</sup> are generally assigned to a trigonal crystal structure containing long continuous chains of Se atoms, while the peaks near and above 250 cm<sup>-1</sup> are generally assigned to monoclinic, orthorhombic and amorphous Se with possible ring configurations and smaller number of Se atoms.<sup>29,30</sup> The detail Raman band assignments are compiled in Table S1. Even though we start with trigonal Se in solid state, which contains continuous long chain of Se atoms, after dissolution of solid, these continuous chains break into smaller polyselenide chains which shifts the Raman band to slightly higher value (~236-246 cm<sup>-1</sup>) than original crystalline trigonal Se band (~234 cm<sup>-1</sup>). For the band near 275 cm<sup>-1</sup>, although second order Raman band for polyselenide chains appear in this range, some cyclic compounds also have calculated Raman bands near 275 cm<sup>-</sup> 1 suggesting a possibility for coexistence of different Se species (chains and rings) in the solution. On the other hand, for Se in EN-ET solution, no peak corresponding to Se-Se bond was observed in the collected spectrum. Instead, the spectrum for this solution showed a very weak intensity peak at 388 cm<sup>-1</sup>, which can be assigned to S-Se bond.31

Although the Raman analysis suggested the formation of different Se compounds in BA-ET versus EN-ET solutions, the <sup>1</sup>H-NMR results obtained for these samples were remarkably similar (Figure S2 and Figure S3). Compared to the pure amine-thiol solutions, both samples exhibited a new quartet and triplet at a δ of 2.72 ppm and 1.28 ppm, respectively, corresponding to the chemical shift of diethyl disulfide (DEDS). Even though there was clear evidence of S-Se interaction in the Raman analysis, no corresponding RSSe signals were observed in the <sup>1</sup>H-NMR spectrum. As the theoretical chemical shifts in the <sup>1</sup>H-NMR for ET and DEDS are similar, it is possible that RSSe and RS ions also have very similar chemical shifts that cannot be distinguished to verify the formation of RSSe in the solution.

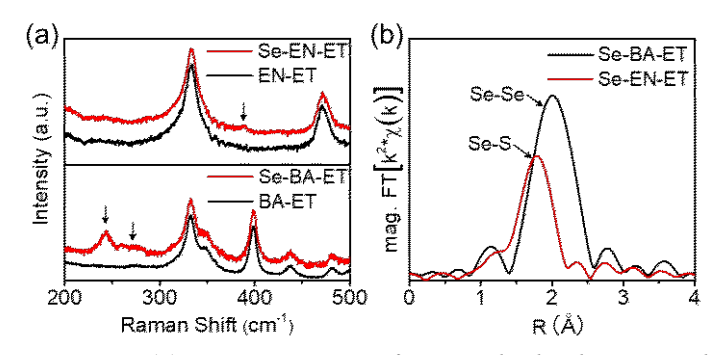


Figure 1: (a) Raman spectra of amine-thiol solutions with and without Se for BA-ET (bottom) and EN-ET (top) systems (b) Se K-edge EXAFS spectra of Se in BA-ET and Se in EN-ET solutions

In order to gain more insight into the complexation and possible bonding in the Se species, X-ray absorption spectroscopy was performed on these two solutions. X-ray absorption is generally used to identify the chemical state through X-ray absorption near edge spectroscopy (XANES) and the coordination environment through extended X-ray absorption fine structures (EXAFS) of a particular metal in the liquid or solid state. The absorption spectra obtained for the Se in BA-ET solution and the Se in EN-ET solution are shown in Figure S4. The XANES analysis indicated that the edge energy of both samples was very close to each other (12.6570 keV and 12.6568 keV) and was lower than that of the Se foil (12.6580 keV). As the edge energies of reference Se compounds containing the -2 oxidation state (In<sub>2</sub>Se<sub>3</sub>, ZnSe) and 0 oxidation state (metallic Se) were very similar, it was difficult to deconvolute the two and assign a specific oxidation state to Se in these solutions. However, the higher white line intensity of the 0.1 M Se solution prepared in BA-ET compared to the 0.1 M Se solution prepared in EN-ET suggests that the local geometry of Se is different in these solutions. After performing the fittings, the Fourier transform of the k<sup>2</sup>-weighted EXAFS of these solutions suggested a significant difference in Se coordination (Figure 1b). As summarized in Table 1, the fitting parameters indeed confirm the different coordinating environment for the two samples.

For Se in BA-ET solution, the parameters obtained from the fitting yielded an average bond distance of 2.34 Å. This bond distance corresponds to a Se-Se bond,<sup>28</sup> confirming the presence of polyselenides in the solution. The bond distance obtained for Se in EN-ET solution was 2.20 Å, which corresponds to the length of a Se-S bonds<sup>28</sup> suggesting the absence of polyselenides and the presence of RSSe species (where R is the thiol alkyl group) in the solution. Average coordination numbers (CN) of 1.6 and 0.8 obtained for Se in BA-ET and EN-ET solutions further support the presence of polyselenides in BA-ET solution and Se terminated RSSe compound in EN-ET solution.

Table 1. Structural parameters obtained from the best fits to Se in BA-ET and Se in EN-ET spectra at the Se

K edge

ix cuge				
Sample	Edge Energy (keV)	Scattering Pair	CN	R (Å)
Se in BA-ET	12.6570	Se-Se	1.6	2.34
Se in EN-ET	12.6568	Se-S	0.8	2.20

After identifying the possible coordination of Se in the BA-ET and EN-ET solutions, further speciation and molecular identification was performed using highresolution ESI-MS analysis. The conditions used for mass spectrometric analysis are detailed in the experimental section. Samples used for this analysis were prepared at a Se concentration of 0.01 M by diluting the solutions with respective amine. Both positive-ion and negative-ion mode ESI-MS spectra were collected, but Se containing species were observed only in negative-ion mode for both samples. The mass spectra measured for the two samples, as shown in Figure 2, look significantly different from each other. The corresponding elemental composition along with the expected error margin are summarized in Table S2. All elemental composition assignments were confirmed using CAD experiments, wherein the fragment ions observed for each ion of interest were consolidated with the elemental composition assignment. The mass spectrum measured for Se in BA-ET (Figure 2, top) revealed ions containing multiple (between one and seven) Se atoms, amongst which HSe<sub>2</sub> ions were the most abundant species. On the other hand, the mass spectrum measured for Se in EN-ET had no HSe<sub>2</sub> ions (Figure 2, bottom), but instead had dominant peak at m/z 141 which correspond to the C<sub>2</sub>H<sub>5</sub>SSe<sup>-</sup> ion. These data confirmed the S-Se bond formation observed for the EN sample in the Raman and XAS analysis. While the mass spectrometry techniques used here analyze the sample in the gas phase and are known to induce some fragmentation and possibly gas phase reactions, 32,33 the results obtained from this analysis agree well with the observations made using other analytical techniques.

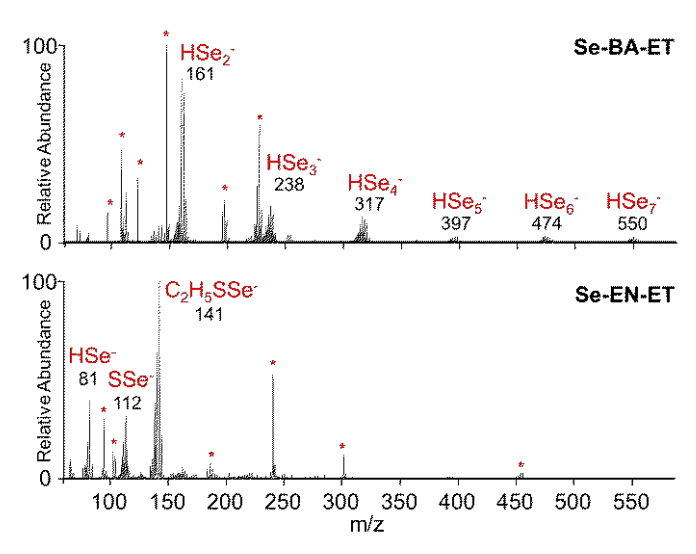


Figure 2: (-) ESI-MS spectra of Se in BA-ET and Se in EN-ET solutions with 1:1 (v/v) amine:thiol (\* peaks without Se atoms)

### **Effects of Thiol Quantity on Selenium Dissolution:**

The analysis of Se-BA-ET and Se-EN-ET solutions suggested the formation of polyselenides with Se-Se bonds in monoamine solutions and RSSe compounds in diamine solutions. These results, particularly in the case of the diamine solution, are not in complete agreement with the previously reported observations by Webber et al., even though some of the analytical techniques used were identical. The main difference between this study and the previous study was identified in the sample preparation. The ratio of amine:thiol (v/v) used in previous study was 4:1 with Se concentration of ~6 M as opposed to amine:thiol (v/v) of 1:1 and Se concentration of 0.1 M used in this study. As various analytical studies performed on amine-thiol solvent system have already shown that this system acts as a reactant rather than just a physical solvent.<sup>24,25</sup> the difference in solute/solvent ratio could impact the species formed in the solution. In this solvent system, for any particular precursor (such as metal salts), the extent of dissolution is associated to the relative amounts of amine and thiol. So, limiting the quantity of either the amine or the thiol generally limits the solubility of the precursor. Such solubility principle has already been utilized by Miskin et al. to demonstrate the varying extent of nucleation in lead chalcogenide nanoparticle synthesis.<sup>22</sup> So, to understand the relation between observed Se species and the solvent ratios used in the solution, an experiment was performed on Se solutions prepared with controlled solvent additions.

To reduce the background signal from the amine-thiol solvent and increase the signal from Se species, new samples with different thiol quantities were prepared at 1.25 M Se concentration instead of 0.1 M. The amount of thiol was varied such that ET:Se mol ratios of 0.3, 0.6, 1.5

and 4 were achieved. To maintain the desired 1.25 M Se concentration, along with variation in the concentration of the thiol, the amine quantities also had to be varied in these samples. Importantly, in all samples, the number of amine groups were always in excess compared to thiol groups, which means that all thiols could theoretically deprotonate in the solution. Two sets of these samples were prepared, one in BA-ET and other in EN-ET solution. From here onwards, the samples discussed in the previous section, that were prepared using 1:1 (v/v) amine:thiol, will be referred to as "excess thiol" samples as the ET:Se mol ratio in those samples was  $\sim$ 69 while among the samples discussed in this section, the one with ET:Se mol ratio of 0.3, will be referred to as "minimum thiol" samples.

Raman analysis performed on the BA-ET samples (Figure 3a) showed similar peaks but with different relative intensities compared to those observed in Figure 1a for Se in BA-ET solution with excess thiol. As can be seen in Figure 3a, the size of the Se-Se bond peak decreased as the thiol quantity increased. Since the total Se concentration, the volume of liquid sample in the cell, and the analysis conditions were all kept constant, the reduction in the intensity of Se-Se bond peak can be associated directly to an actual reduction in the number of Se-Se bonds in the sample. With increasing thiol quantity, the shift of 236 cm<sup>-</sup> <sup>1</sup> peak towards higher frequencies support the reduction in the number of Se-Se bonds due to a transition from long chain polyselenides to short chain polyselenides. Also the presence of two distinct peaks for the sample with ET:Se of 0.3 suggests the possibility for co-existence of linear and cyclic polyselenide compounds as the A1 mode Raman band for cyclic Se<sub>6</sub> and Se<sub>8</sub> compounds are at ~ 247 cm<sup>-1</sup> and 250 cm<sup>-1</sup> respectively.

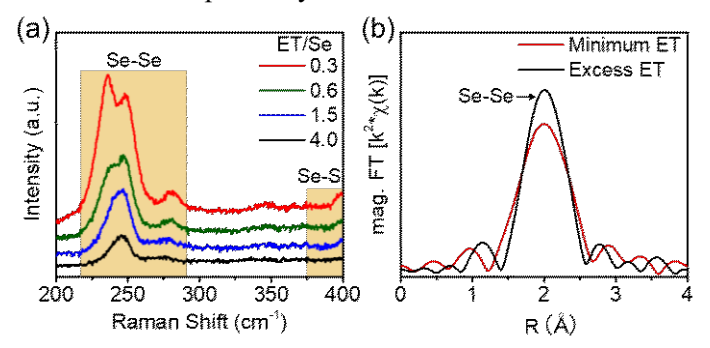


Figure 3: (a)Raman spectra of Se in BA-ET solutions with varying quantity of ET (b) the magnitude component of the Fourier transforms (FTs) of Se K-edge k2-weighted EXAFS spectra measured for Se in BA-ET solutions with minimum ET and excess ET used for dissolution

In order to further understand the difference with thiol variation, the XAS analysis was performed on Se in BA-ET solution with minimum thiol (Figure S6). Fittings performed on EXAFS of collected absorption data also showed the presence of only Se-Se bonds with an average

bond distance of 2.35 Å and an absence of S-Se interaction in the solution (Figure 3b). While similar atomic interactions were observed for Se in BA-ET solutions for excess and minimum thiol quantities, the average CN obtained for these two samples did vary slightly.

The CN obtained for the sample with the minimum thiol (1.8) was 0.2 greater than that obtained for the sample with excess thiol (1.6). This increase in CN can be attributed to longer chain length of polyselenides or coexistence of cyclic polyselenides. In cyclic polyselenides, every selenium will have CN of 2, so their co-existence could increase the average CN of Se in the solution. Similarly, in linear chain structures, all the Se atoms within the chain have CN of two but the two terminal atoms in the chain have the CN of one, giving an average CN of Se atoms less than two. In the case of long chain structures, the Se atoms with a CN of two are more in number when compared to short chain structures, resulting in a slightly higher average CN than the one for short chain structures. Based on this analysis, it was proposed that the polyselenides (Se<sub>x</sub>) decrease in size (average x decreases) with increasing thiol quantity in the solution.

To identify the average number of Se atoms in polyselenides (value of x) formed in the solution, <sup>1</sup>H-NMR analysis was performed on Se in BA-ET solutions with different thiol quantities (Figure S7). Interestingly, with increasing thiol quantity, the amount of DEDS formed in the solution was also increased (integration of H<sub>b</sub> protons in Figure S7). When quantified with <sup>1</sup>H-NMR using ethylene carbonate as the NMR standard, the amount of DEDS in the solution was found to increase in first three samples with increasing thiol (ET/Se ratio of 0.3, 0.6 and 1.5) but stayed the same when more thiol was added (ET/Se of 4) in the solution. As the formation of DEDS molecules results from combining two thiolate ions by losing two electrons  $(2mRS^{-} \rightarrow mRSSR + 2me^{-})$ , the formation of m moles of DEDS suggests transfer of 2m electrons to polyselenides. If we assume identical polyselenides are formed in the solution (i.e. only one value of x for all  $Se_x^{2-}$ ) from initial n moles of Se, we will have a relation: nSe +  $2\text{me}^{-} \rightarrow \text{mSe}_{x}^{2-}$ . As n is known from starting Se quantity and m can be obtained from the quantitative <sup>1</sup>H-NMR by integrating protons corresponding to DEDS, average value of x can be derived using x=n/m. On average, the quantitative NMR suggested the formation Se<sub>6.25</sub><sup>2-</sup>, Se<sub>5.35</sub><sup>2-</sup>, and Se<sub>3.95</sub><sup>2-</sup> species for samples with ET/Se ratio of 0.3, 0.6 and 1.5 respectively. Since the further addition of thiol did not result in additional DEDS formation, Se<sub>3.95</sub><sup>2-</sup> appears to smallest average size of polyselenide species present in the solution. Note that these calculations are based on average values, so the actual polyselenides will contain a whole number of Se atoms instead of fractions (i.e., Se4 instead of Se<sub>3.95</sub>). Although the average number of Se atoms in polyselenides is four, the solution will likely have some polyselenides with more than four Se atoms while others with less than four Se atoms

To explore the differences in the species in two solutions, ESI-MS analysis was performed on the Se in BA-ET sample with minimum thiol and then compared to the Se in BA-ET sample with excess thiol (Figure S8). The results showed considerable differences between the two solutions. For the minimum thiol sample, the sizes of the HSe<sub>x</sub> ion observed in the ESI mass spectrum varied from HSe<sub>2</sub><sup>-</sup> to HSe<sub>7</sub><sup>-</sup>. While these same ions were observed in the mass spectrum measured for the sample with excess thiol, the relative abundances of the larger HSe<sub>x</sub><sup>-</sup> ions were much smaller. This finding supports the NMR, Raman, and XAS data, suggesting that in minimum thiol samples, longer polyselenides are favored and with thiol addition, these long chain polyselenides transform to smaller chains. Although in low abundance, an interesting observation made for Se in the BA-ET solution with minimum thiol was the presence of RSSe<sup>-</sup> species in the mass spectra. Since no S-Se interaction was identified through Raman or XAS analysis of this solution, it is hypothesized that the presence of longer polyselenides initiate the interactions with RSions in the mass spectrometer ion source. The reasons for this behavior are still unclear.

Since the samples analyzed for studying the effect of thiol variation were prepared at 1.25 M Se concentration which is ~10 times concentrated compared to samples analyzed in previous section, the effect of Se concentration on the species formed was also studied for these solutions using Raman analysis. The samples with different Se concentrations (1.25 M, 0.1 M, 0.01 M) were prepared by either keeping ET:Se mol ratio fixed at 0.3 (addition of amine for dilution) or by keeping BA:ET mol ratio fixed at 5 (addition of amine and thiol for dilution). The Raman spectra collected for solutions prepared with amine dilution (fixed ET:Se ratio) showed presence of two identical peaks at different concentrations, while the spectra collected for solutions prepared with amine-thiol dilution (fixed amine:thiol ratio) showed presence of one peak corresponding to polyselenide species for all concentrations (Figure S5). These results suggest that Se concentration when varied within 0.01 M to 1.25 M range doesn't have as significant effect on the species as the thiol: Se ratio in the solution.

After analyzing effect of thiol variation on Se species in BA-ET solutions, similar study was performed for EN-ET solutions. The Raman spectra measured for Se in EN-ET solutions with varying thiol quantities (Figure 4a) showed different peaks compared to those observed in Figure 1a for Se in EN-ET with excess thiol. The major difference was the presence of Se-Se bonds in all four

samples, which was missing from the excess thiol spectrum. Additionally, the four samples themselves showed variations in their Raman spectra as the thiol quantity was increased. The first two samples with ET/Se ratios of 0.3 and 0.6 showed a complete absence of S-Se bonds. With increasing thiol, S-Se bonds began to appear in the Raman spectrum with simultaneous reduction in the size of the Se-Se bond peak. Similar to the observations made for Se in BA-ET, as the thiol quantity was increased, the Se-Se bond characteristics transitioned from long chain polyselenides to short chain polyselenides with fewer Se-Se interactions. <sup>1</sup>H-NMR analysis performed on all four samples showed peaks corresponding to DEDS (Figure S9). A quantitative analysis, similar to the one described for BA-ET solution, was performed on the EN-ET samples with different thiol quantities. The results suggest the formation of Se<sub>6.82</sub><sup>2-</sup>, Se<sub>6.25</sub><sup>2-</sup>, Se<sub>3.95</sub><sup>2-</sup> and Se<sub>3.65</sub><sup>2-</sup> polyselenides for samples with ET:Se of 0.3, 0.6, 1.5 and 4, respectively.

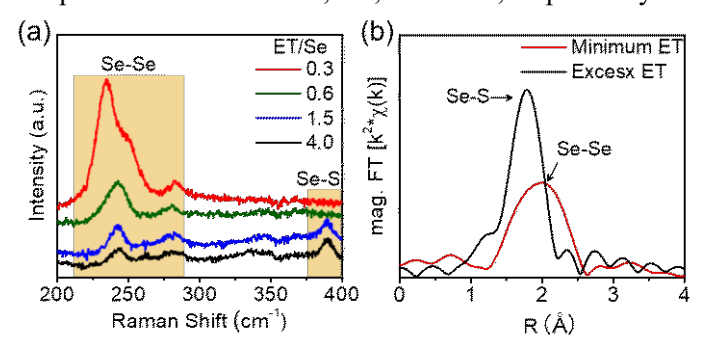


Figure 4: (a) Raman spectra of Se in EN-ET solutions with varying quantity of ET (b) the magnitude component of the Fourier transforms (FTs) of Se K-edge k2-weighted EXAFS spectra measured for Se in EN-ET solutions with minimum ET and excess ET used for dissolution

The observations made for Se in solutions containing different thiol quantities were further confirmed with XAS analysis. No Se-Se peak was observed for the Se in EN-ET solution with excess thiol. However, the minimum thiol quantity sample showed only Se-Se interactions with a bond distance of 2.35 Å (Figure 4b), supporting the findings from the Raman analysis. Unlike Se in BA-ET solutions, the mass spectra obtained for Se in EN-ET with minimum and excess thiol quantities were vastly different from one another (Figure S8 and Table S3). The ions identified in the mass spectrum for Se in EN-ET with minimum thiol were similar to those observed in the mass spectra collected for Se in BA-ET solutions. Polyselenides ranging from HSe<sub>2</sub><sup>-</sup>up to HSe<sub>6</sub><sup>-</sup>, in addition to several RSSe<sup>-</sup> ions, including ETSe<sup>-</sup>, ETSe<sub>2</sub><sup>-</sup>, and ETSe<sub>3</sub><sup>-</sup> were observed in the mass spectrum. For the excess thiol sample, however, the polyselenides were entirely absent, with the most abundant peak at m/z 141 corresponding to the ETSe<sup>-</sup>ion. It is possible that longer polyselenides exist in the excess thiol solution, but in concentrations lower than the detection

limit of the mass spectrometer. However, these findings confirm the transition from  $Se_x^{2-}$  to  $RSSe^-$  compounds with increasing thiol quantities.

Scheme 1: Proposed reaction pathway for dissolution of Se in monoamine and diamine solutions with gradual thiol addition.

### Monoamine-Monothiol

$$\begin{array}{c} 2mRS^{\text{-}} \\ nSe \overset{}{\longrightarrow} mRSSR + \sum\limits_{j=1}^{p} m_{j} Se_{x_{j}^{2^{\text{-}}}} \left[ \sum\limits_{\substack{j=1 \\ p = 1}}^{p} m_{j} x_{j} = n \right] .... \text{Overall reaction} \\ \\ 2RS^{\text{-}} \\ nSe \overset{}{\longrightarrow} RSSR + (n-x)Se + \frac{2}{Se_{x}^{2^{\text{-}}}} \overset{}{\longrightarrow} RSSR + \frac{2}{Se_{x}^{2^{\text{-}}}} + \frac{2}{Se_{x}^{2^{\text{-}}}} \\ \end{array}$$

#### Diamine-Monothiol

$$2mRS^{-}$$
 $nSe \longrightarrow (m-n/2)RSSR + nRSSe^{-}$ 
....Overall reaction
$$2RS^{-}$$
 $nSe \longrightarrow RSSR + (n-x)Se + Se_{x}^{2-} \longrightarrow 2RSSe_{y}^{-} + Se_{x,2y}^{2-}$ 

Based on these observations, the Scheme 1 shows the difference in the species formed in the monoamine vs diamine solutions. In the case of the monoamine, initial thiol addition starts the dissolution of Se through disulfide formation and electron transfer to form polyselenide ions. After complete dissolution of Se in the solution, further thiol addition results in additional thiol deprotonation. which drives the continued donation of electrons to polyselenide ions, making smaller polyselenide ions containing fewer Se atoms. Once the polyselenide ions reach a certain size, the transfer of electrons from RS- to polyselenide ions is no longer favorable. This could be a result of competing nucleophilicity between the RS and polyselenide ion in the presence of a monoammonium cation. For the diamine, similar to monoamine, initial thiol addition leads to Se dissolution through disulfide and polyselenide ion formation. However, further thiol addition continues to make smaller polyselenide ions along with thiol-coordinated polyselenides ions (RSSe<sub>y</sub>-), eventually forming mono-selenium thiolate (RSSe<sup>-</sup>). This difference in two solutions could be a result of different nucleophilic interactions in diammonium cation solutions compared to monoammonium cation solutions. One could also attribute the difference in BA and EN dissolutions to the chelating nature of EN providing possible intermediate pathway for Se-EN coordination. 34,35 But lack of evidence and literature guidance make the understanding of overall role of amines in these dissolutions unclear.

#### **Tellurium Dissolutions in Diamine Solutions:**

Similar to Se, Te dissolves in diamine-thiol solutions, but the solubility limit for Te in the EN-ET solution at room temperature is very low (~0.6 M) compared to that of Se (~6 M).<sup>15</sup> The EN-ET solution of Te also behaves differently from the EN-ET solution of Se when the solvent is evaporated at ambient temperature. Unlike the EN-ET solution of Se, which gives a stable Se complex after removing the thiol and amine from the solution, removing the solvent from the EN-ET solution of Te results in precipitation of metallic Te.<sup>15</sup> These behaviors suggest that different Se and Te species are formed in the EN-ET solution.

To examine the species formed during Te dissolution, Raman analysis was performed on a 0.5 M EN-ET solution of Te with 1:1 volume ratio of EN:ET (ET:Te mol ratio = 13.86) and was compared with the Raman spectrum collected for metallic Te powder (Figure 5a). The spectrum measured for the powdered tellurium sample showed two peaks between 100-150 cm<sup>-1</sup> which correspond to crystalline Te-Te interactions. 36,37 However, the spectrum measured for the solution of Te in the EN-ET solvent showed multiple peaks in the range of 150-200 cm<sup>-1</sup> but none in 100-150 cm<sup>-1</sup>, suggesting an absence of crystalline Te in the solution. Based on previous reports, the Raman shift between 150-175 cm<sup>-1</sup> corresponds to amorphous Te, which suggests the presence of low order Te-Te interactions in the solution. 36,37 Similar to the Se in EN-ET solution, the Raman spectrum measured for Te in EN-ET also showed the presence of Te interactions with sulfur, as the peak in the range of 175-200 cm<sup>-1</sup> was assigned to Te-S bonds.<sup>38,39</sup> This observed bonding from Raman analysis was further confirmed via XAS experiment performed at Te K edge. Fittings performed on EXAFS of collected absorption data (Figure 5b and Figure S10) showed the presence of Te-Te bonds having an average bond distance of 2.73 Å with C.N of 1.7 and Te-S bonds with an average bond distance of 2.42 Å and C.N of 0.4. Since the solubility limit of Te is very low, the least amount of thiol required for dissolution of 0.5 M Te in EN-ET solution yields a ET:Te mol ratio of around 4. Any further addition of thiol into this solution simply resulted in dilution of the Te solution without any detectable changes in bonding. This suggests, unlike Se dissolution in EN-ET solution (containing excess thiol) which results in RSSe-ions with no Se-Se interaction, Te-EN-ET solution always contains Te-Te interaction.

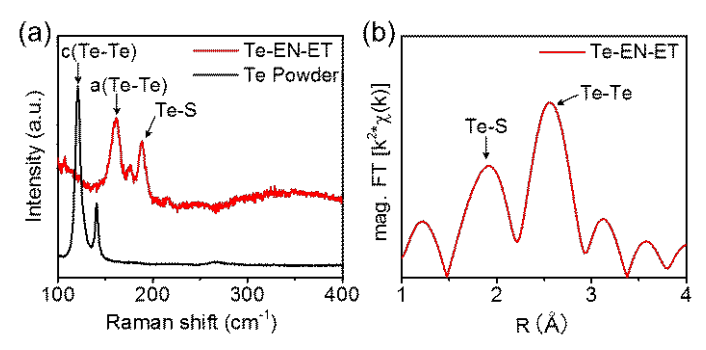


Figure 5: (a) Raman spectra of metallic Te powder and Te in EN-ET solution (c(Te-Te): crystalline Te-Te interaction, a(Te-Te): amorphous Te-Te interaction) (b) the magnitude component of the Fourier transforms (FTs) of Te K-edge k2-weighted EXAFS spectra measured for Te in EN-ET solution

Similar to Se solutions, identification of Te species was realized using ESI-MS analysis and the Te-containing compounds were only ionized when using negative mode of ESI-MS. Qualitatively, the mass spectrum of Te in EN-ET solution (Figure 6 and Table S4) looked very similar to the mass spectrum of Se in EN-ET with minimum thiol. ETTe<sup>-</sup> and ETTe<sub>2</sub><sup>-</sup>, were the most abundant ions in the mass spectrum, while ETTe<sub>3</sub>- species were also observed with very small relative abundance. Additionally, HTe<sub>x</sub> ions similar to HSe<sub>x</sub> ions were also observed, with x ranging from two to four (two being most abundant). Previous mass spectrometric studies<sup>40</sup> of Te have concluded that gas-phase tellurium is most stable as Te2, which supports our observations. However, these thiol free polytellurides could be an artifact of the ESI source and not necessarily present in the solution. As Te tends to precipitate out as metallic Te with solvent evaporation, during ESI process, it is very likely for Te to partially precipitate out and appear as thiol free polytelluride ion in the spectrum.

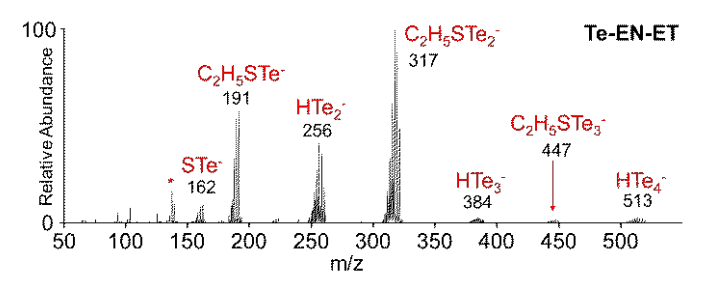


Figure 6: (-) ESI-MS spectrum of Te in EN-ET solution (\* peaks without Te atoms)

### Co-dissolution of Tellurium and Selenium:

Dissolutions of Se and Te performed individually in the EN-ET solution suggest some similarities and some differences in the species formed in solution. Although Se and Te are in same group of the periodic table and both naturally occur as trigonal crystal structures, the properties

of their crystal structures are somewhat different. For example, the atomic interactions within the crystal structures varies for Se and Te. In the trigonal structure, atoms are connected in long cross-linked chains. In the Se trigonal structure, the interaction of atoms within a single chain are much stronger than the interaction of atoms between two adjacent chains, making it easy to separate two chains from each other. On the other hand, in the Te crystal structure, the interaction of atoms in neighboring chains is just as strong as the attraction of atoms within a single chain. 40 This difference can play an important role not only in chalcogen dissolution but also in its recovery from the solution, resulting in some dissimilarities for the two chalcogen solutions. While Te is known to have a solubility limit of 0.6 M in EN-ET solutions, it is observed that it could be dissolved at higher concentrations in the presence of Se. Additionally, unlike the evaporation of EN-ET solvent from Te solution, which results in the metallic precipitation of Te, the evaporation of the EN-ET solvents from co-dissolved Se and Te solution did not result in precipitation of metallic tellurium. Instead, a stable organometallic complex was formed in the solution. These observations suggest that in the presence of Se, Te forms a different species in solution with different properties than the ones when it is dissolved independently.

To confirm the presence of new species formation, a solution of Se and Te (Se:Te = 7:3) in EN-ET was analyzed via various techniques. The Raman spectrum measured for this solution, shown in Figure 7a, suggests the presence of Se-Se bonds, Te-Te bonds, and an additional bond type resulting in a broad peak between 175-225 cm<sup>-1</sup>. Although a Raman shift of S-Te bonds occurs in this range, it could also be assigned as a Raman shift for Se-Te bonds due to the broadening of the peak.<sup>41,42</sup>

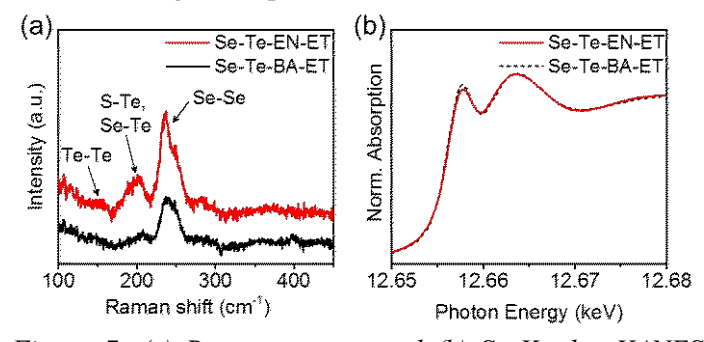


Figure 7: (a) Raman spectra and (b) Se K-edge XANES spectra of Se and Te codissolved in BA-ET and EN-ET solutions

To further verify the multiple interactions, XAS analysis was performed on above solution at the Se edge (Figure 7b and Figure S11). Fitting performed on these data confirmed the presence of S-Se, Se-Se, and Se-Te bonds with a total CN of around two (Table 2). After confirming the presence of multiple interactions, this solution was

analyzed using ESI-MS to identify the chemical formulas of the species which suggested the formation of a wide variety of compounds, including: RSSe<sub>x</sub>, RSTe<sub>y</sub>, RSSe<sub>x</sub>Te<sub>y</sub> and Se<sub>x</sub>Te<sub>y</sub> (Figure 8 and Table S5). These structures also support the assignment of the Raman broad peak between 175-225 cm<sup>-1</sup> to both S-Te and Se-Te bonds.

Table 2. Structural parameters obtained from the best fits to Se-Te-BA-ET and Se-Te in EN-ET spectra at the Se K edge

Sample	Edge energy (keV)	Scattering Pair	CN	R (Å)
Se-Te-	12 (5(2	Se-Se	0.4	2.34
BA-ET	12.6562	Se-Te	1.4	2.48
Se-Te in		Se-S	0.6	2.31
EN-ET	12.6562	Se-Se	0.7	2.34
EIN-E I		Se-Te	0.7	2.48

The presence of Se<sub>x</sub>Te<sub>y</sub> compounds in the solution suggests a different dissolution route for Te in the presence of Se. The Sex<sup>2-</sup> ion formed in the solution may act as a nucleophile similar to the RS<sup>-</sup> ion, resulting in dissolution of Te through the formation of Se<sub>x</sub>Te<sub>y</sub> complexes. This hypothesis was explored by testing whether the presence of Se can make Te soluble in a BA-ET solution, where Te is otherwise insoluble. Sex<sup>2-</sup> ions were generated in BA-ET solution by dissolving Se in the solvent as previously described. Then, Te was added and the solubility of Te in the resulting solution was tested. This experiment indeed resulted in the incorporation of Te into the BA-ET solution. Raman (Figure 7a) and XAS analysis (Table 2) performed on this solution confirmed the formation of Se-Te bonds along with Se-Se bonds. Mass spectrometry measurements of this solution also support the formation of Se<sub>x</sub>Te<sub>y</sub> compounds. Unlike the EN-ET solution of codissolved Se and Te, in the BA-ET solution, Se<sub>x</sub>Te<sub>y</sub> ions were present almost exclusively without thiol interactions. Additionally, no evidence for S-Te interactions were found suggesting that the only mechanism of Te dissolution involves complexing with Se in this solution (Figure 8). Interestingly, the relative number of Te atoms in these Se<sub>x</sub>Te<sub>y</sub> ions was found to be always less than or equal to the number of Se atoms in the same ion (i.e. x>y). This sets a possible solubility limit on Te dissolution in BA-ET. Although various values of x and y in the Se<sub>x</sub>Te<sub>y</sub> compound were discovered using mass spectrometry experiments, the maximum ratio of Te:Se that could be dissolved in BA-ET solvent was found to be 2:3. This result suggests that on average, molecule containing three atoms of Se can coordinate with and dissolve up to two Te atoms.

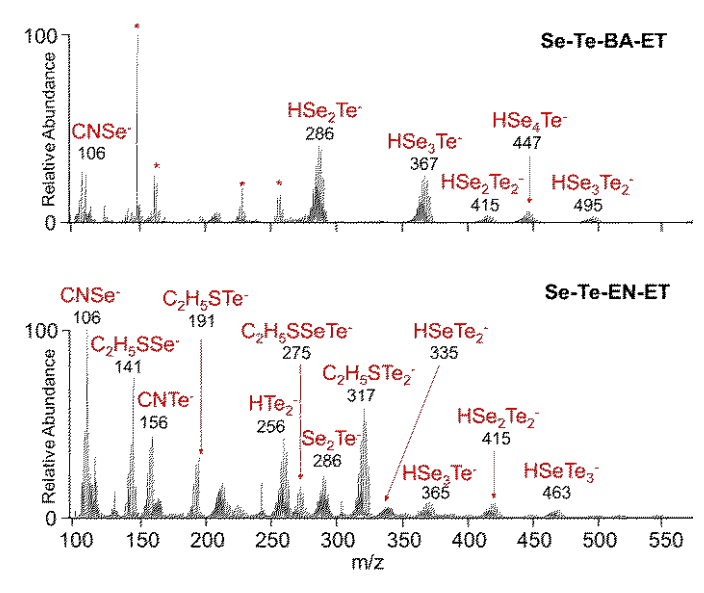


Figure 8: (-) ESI-MS spectra of Se and Te in BA-ET and Se and Te in EN-ET solutions (\* peaks without Se/Te atoms)

# Tuning Material Synthesis through Discovered Chemical Understanding:

The new understanding of the species formed in aminethiol solvents can be applied to various material synthesis, especially for the synthesis of metal chalcogenides. Our previous work on the synthesis of lead chalcogenide particles showed some particle morphology variations when the solvent was changed from monoamine-thiol to diamine-thiol.<sup>22</sup> The findings from this study on Se and Te species identification have now provided a preliminary reasoning behind the differences observed in the material synthesis. It also provided a better route to control and tune the properties of the resulting materials.

To demonstrate one among many other possible utilities of the findings made in this study, two solutions containing co-dissolved Se and Te were used for synthesis of PbSe<sub>n</sub>Te<sub>1-n</sub> materials. Se and Te (4:1 mol ratio) were dissolved in a 1:1 (v/v) BA-ET solution and a 1:1 (v/v) EN-ET solution. Based on our analysis, the BA-ET solution contains mainly Se<sub>x</sub>Te<sub>y</sub> species while the EN-ET solution contains a variety of species, including RSSex, RSTex, RSSe<sub>x</sub>Te<sub>y</sub> and Se<sub>x</sub>Te<sub>y</sub>. Although both inks were prepared with the same quantities of chalcogen, the differences observed in the chalcogen complexes could affect the reactivity of each solution. For the EN-ET solution containing both Se and Te, each of the proposed chalcogen complexes such as RSSe<sub>x</sub>, RSTe<sub>x</sub> etc. in this solution may react independently, affecting the overall material synthesis. To test this hypothesis, these two solutions (Se-Te-BA-ET and Se-Te-EN-ET) were allowed to react at room temperature with a lead acetate solution prepared in pure EN to form a lead chalcogenide material. These reactions resulted in instant precipitation of particles from the solution. The particles were washed and analyzed using scanning electron microscopy (SEM), X-ray fluoroscence (XRF), and X-ray diffraction (XRD) techniques to study the material properties. The SEM images for both the materials suggest formation of nanoparticles with particle size in the range of few tens of nanometers (Figure S12). Based on the elemental composition obtained from XRF data, no sulfur was detected in the particles and the ratio of Se/(Se+Te) was calculated to be 0.22 and 0.21 for BA-ET and EN-ET synthesized PbSe<sub>n</sub>Te<sub>1-n</sub> particles respectively which is close to the starting value of 0.20 in the solution. Although the elemental composition for both materials was similar, the XRD patterns for these two materials were different. As can be seen in Figure 9, for the  $2\theta$  at approximately 28°, the XRD pattern collected for the material formed in the EN-ET solution had two different broad peaks, one corresponding to Se rich PbSe<sub>n</sub>Te<sub>1-n</sub> and another corresponding to Te rich PbSe<sub>n</sub>Te<sub>1-n</sub>. On the other hand, the material synthesized from the BA-ET solution had only one broad peak, confirming a uniformly alloyed PbSe<sub>n</sub>Te<sub>1-n</sub> material. This experiment shows that by carefully choosing the composition of the amine-thiol solvent, one can control the properties of a synthesized material.

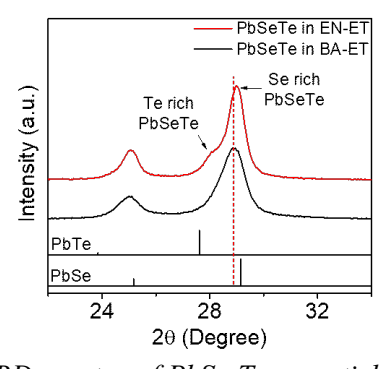


Figure 9: XRD spectra of  $PbSe_nTe_{1-n}$  particles synthesized using BA-ET and EN-ET solutions of Se and Te

### **Conclusions:**

In this work, Raman spectroscopy, X-ray absorption spectroscopy, high-resolution tandem mass spectrometry, and <sup>1</sup>H-NMR spectroscopy were used to analyze chalcogen dissolution in amine-thiol solutions. This analysis suggest that, the species formed in solution can vary significantly based on whether the amine used is a monoamine or a diamine. When dissolved in monoamine-thiol solutions, Se formed polyselenides ions while in diamine-thiol solutions, Se formed polyselenides that were coordinated with thiols. Additionally, the quantity of thiol used for dissolution affected the Se species formed in the solution, with increasing amounts of thiol resulting in a shift from long chain polyselenides to smaller polyselenides. In diaminethiol solution containing much excess thiol, the dominant Se species was observed to be mono-selenium thiolate. Te, which dissolves only in dimine-thiol solutions, was also

found to form thiol-cordinated polytellurides. However, unlike polyselenides, these polytellurides are highly unstable, resulting in metallic tellurium precipitaion with solvent evaporation or foreign solvent addition. The dissolution of Te was futher analyzed in the presence of Se. The two chalcogens were found to interact in the aminethiol solution, forming various compounds containing Se-Te bonds. This finding was then utilized to demonstrate the dissolution of Te in monoamine-thiol solution in the presence of the Se<sub>x</sub><sup>2</sup>- nucleophile. The chalcogen species formed under different amine-thiol conditions were then utilized to demonstarte composition control with Pb chalcogenide material synthesis. The chalcogen incorporation during such material synthesis was successfully controlled through the appropriate selection of the chalcogen species. Similar to lead chalcogenide synthesis, the findings from this study can be further applied for controlling chalcogen behavior during a variety of metal chalcogenide synthesis where an amine-thiol is used as the solvent system.

# **Supporting Information:**

Raman spectra of Se powder and Se-BA-ET solutions at different concentrations, NMR spectra for Se-BA-ET and Se-EN-ET solutions, XAS spectra, Mass spectra for Se solutions with minimum thiol, tables with m/z assignments for mass spec results, SEM images of PbSe<sub>n</sub>Te<sub>1-n</sub> particles

# **Acknowledgment:**

SDD and KGW would like to acknowledge the funding support provided by the National Science Foundation under grant #1534691-DMR (DMREF) and grant #1735282-NRT (SFEWS) respectively. Authors would also like to acknowledge Johnny Zhuchen for his help with X-ray absorption experiments and Judy Kuan-Yu Liu for discussions regarding mass spectrometry experiments. Use of the Advanced Photon Source was supported by the U.S. Department of Energy Office of Basic Energy Sciences under contract no. DE-AC02-06CH11357. MRCAT operations, beamlines 10-BM and 10-ID, are supported by the Department of Energy and the MRCAT member institutions. RA would also like to acknowledge the support provided by NSF grant #10001536 (INFEWS).

### **References:**

- (1) Gao, M.-R.; Xu, Y.-F.; Jiang, J.; Yu, S.-H. Nanostructured Metal Chalcogenides: Synthesis, Modification, and Applications in Energy Conversion and Storage Devices. *Chem. Soc. Rev.* **2013**, *42* (7), 2986.
- (2) Huang, W.; Gan, L.; Li, H.; Ma, Y.; Zhai, T. 2D Layered Group IIIA Metal Chalcogenides: Synthesis, Properties and Applications in

- Electronics and Optoelectronics. *CrystEngComm* **2016**, *18* (22), 3968–3984.
- (3) García de Arquer, F. P.; Armin, A.; Meredith, P.; Sargent, E. H. Solution-Processed Semiconductors for next-Generation Photodetectors. *Nat. Rev. Mater.* **2017**, *2* (3), 16100.
- (4) Abbel, R.; Galagan, Y.; Groen, P. Roll-to-Roll Fabrication of Solution Processed Electronics. *Adv. Eng. Mater.* **2018**, *20* (8), 1701190.
- (5) Habas, S. E.; Platt, H. A. S.; Van Hest, M. F. A. M.; Ginley, D. S. Low-Cost Inorganic Solar Cells: From Ink to Printed Device. *Chem. Rev.* 2010, 110 (11), 6571–6594.
- (6) Azimi, H.; Brabec, C. J. Towards Low-Cost, Environmentally Friendly Printed Chalcopyrite and Kesterite Solar Cells. *Energy Environ. Sci.* **2014**, 7, 1829–1849.
- (7) Uhl, A. R.; Katahara, J. K.; Hillhouse, H. W. Molecular-Ink Route to 13.0% Efficient Low-Bandgap CuIn(S,Se)<sub>2</sub> and 14.7% Efficient Cu(In,Ga)(S,Se)<sub>2</sub> Solar Cells. *Energy Environ. Sci.* **2016**, *9* (1), 130–134.
- (8) Yuan, M.; Mitzi, D. B. Solvent Properties of Hydrazine in the Preparation of Metal Chalcogenide Bulk Materials and Films. *Dalt. Trans.* **2009**, *31* (31), 6078.
- (9) Murray, C. B.; Norris, D. J.; Bawendi, M. G. Synthesis and Characterization of Nearly Monodisperse CdE (E = Sulfur, Selenium, Tellurium) Semiconductor Nanocrystallites. *J. Am. Chem. Soc.* **1993**, *115* (19), 8706–8715.
- (10) Peng, X.; Wickham, J.; Alivisatos, A. P. Kinetics of II-VI and III-V Colloidal Semiconductor Nanocrystal Growth: "Focusing" of Size Distributions. *J. Am. Chem. Soc.* **1998**, *120* (21), 5343–5344.
- (11) Klayman, D. L.; Griffin, T. S. Reaction of Selenium with Sodium Borohydride in Protic Solvents. A Facile Method for the Introduction of Selenium into Organic Molecules. *J. Am. Chem. Soc.* **1973**, *95* (1), 197–199.
- (12) Webber, D. H.; Brutchey, R. L. Alkahest for V2VI3 Chalcogenides: Dissolution of Nine Bulk Semiconductors in a Diamine-Dithiol Solvent Mixture. J. Am. Chem. Soc. 2013, 135 (42), 15722–15725.
- (13) Zhang, R.; Szczepaniak, S. M.; Carter, N. J.;

- Handwerker, C. A.; Agrawal, R. A Versatile Solution Route to Efficient Cu<sub>2</sub>ZnSn(S,Se)<sub>4</sub> Thin-Film Solar Cells. *Chem. Mater.* **2015**, *27* (6), 2114–2120.
- (14) Zhang, R.; Cho, S.; Lim, D. G.; Hu, X.; Stach, E. A.; Handwerker, C. A.; Agrawal, R. Metal-metal Chalcogenide Molecular Precursors to Binary, Ternary, and Quaternary Metal Chalcogenide Thin Films for Electronic Devices. *Chem. Commun.* 2016, 846 (1–4), 31–39.
- (15) Webber, D. H.; Buckley, J. J.; Antunez, P. D.; Brutchey, R. L. Facile Dissolution of Selenium and Tellurium in a Thiol–amine Solvent Mixture under Ambient Conditions, *Chem. Sci.* **2014**, *5* (6), 2498.
- (16) Walker, B. C.; Agrawal, R. Contamination-Free Solutions of Selenium in Amines for Nanoparticle Synthesis. *Chem. Commun.* **2014**, *50* (61), 8331.
- (17) McCarthy, C. L.; Brutchey, R. L. Solution Processing of Chalcogenide Materials Using Thiol–amine "alkahest" Solvent Systems. *Chem. Commun.* **2017**, *53* (36), 4888–4902.
- (18) Zhao, X.; Lu, M.; Koeper, M.; Agrawal, R. Solution-Processed Sulfur Depleted Cu(In,Ga)Se<sub>2</sub> Solar Cells Synthesized from a Monoamine-Dithiol Solvent Mixture. *J. Mater. Chem. A* **2016**, *4* (19), 7390–7397.
- (19) Yu, X.; Cheng, S.; Yan, Q.; Yu, J.; Qiu, W.; Zhou, Z.; Zheng, Q.; Wu, S. Efficient (Cu<sub>1-x</sub>Ag<sub>x</sub>)<sub>2</sub>ZnSn(S,Se)<sub>4</sub> Solar Cells on Flexible Mo Foils. *RSC Adv.* **2018**, 8 (49), 27686–27694.
- (20) Miskin, C. K.; Dubois-Camacho, A.; Reese, M. O.; Agrawal, R. A Direct Solution Deposition Approach to CdTe Thin Films. *J. Mater. Chem. C* **2016**, *4* (39), 9167–9171.
- (21) McCarthy, C. L.; Brutchey, R. L. Solution Deposited Cu<sub>2</sub>BaSnS<sub>4-x</sub>Se<sub>x</sub> from a Thiol-Amine Solvent Mixture. *Chem. Mater.* **2018**, *30* (2), 304–308.
- (22) Miskin, C. K.; Deshmukh, S. D.; Vasiraju, V.; Bock, K.; Mittal, G.; Dubois-camacho, A.; Vaddiraju, S.; Agrawal, R. Lead Chalcogenide Nanoparticles and Their Size-Controlled Self-Assemblies for Thermoelectric and Photovoltaic Applications. ACS Appl. Nano Mater. 2019, 2, 1242–1252.
- (23) Deshmukh, S. D.; Ellis, R. G.; Sutandar, D. S.; Rokke, D. J.; Agrawal, R. Versatile Colloidal Syntheses of Metal Chalcogenide Nanoparticles

- from Elemental Precursors Using Amine-Thiol Chemistry. *Chem. Mater.* **2019**, *31* (21), 9087–9097.
- (24) Murria, P.; Miskin, C. K.; Boyne, R.; Cain, L. T.; Yerabolu, R.; Zhang, R.; Wegener, E. C.; Miller, J. T.; Kenttämaa, H. I.; Agrawal, R. Speciation of CuCl and CuCl<sub>2</sub> Thiol-Amine Solutions and Characterization of Resulting Films: Implications for Semiconductor Device Fabrication. *Inorg. Chem.* 2017, 56 (23), 14396–14407.
- (25) Zhao, X.; Deshmukh, S. D.; Rokke, D. J.; Zhang, G.; Wu, Z.; Miller, J. T.; Agrawal, R. Investigating Chemistry of Metal Dissolution in Amine–Thiol Mixtures and Exploiting It toward Benign Ink Formulation for Metal Chalcogenide Thin Films. *Chem. Mater.* 2019, 31 (15), 5674–5682.
- (26) Walker, B.; Agrawal, R. Grain Growth Enhancement of Selenide CIGSe Nanoparticles to Densified Films Using Copper Selenides. *Conf. Rec. 38th IEEE Photovolt. Spec. Conf.* 2012, 2654–2657.
- (27) Liu, Y.; Yao, D.; Shen, L.; Zhang, H.; Zhang, X.; Yang, B. Alkylthiol-Enabled Se Powder Dissolution in Oleylamine at Room Temperature for the Phosphine-Free Synthesis of Copper-Based Quaternary Selenide Nanocrystals. *J. Am. Chem. Soc.* **2012**, *134* (17), 7207–7210.
- (28) Allen, F. H.; Kennard, O.; Watson, D. G.; Brammer, L.; Orpen, A. G.; Taylor, R. Tables of Bond Lengths Determined by X-Ray and Neutron Diffraction. Part 1. Bond Lengths in Organic Compounds. *J. Chem. Soc. Perkin Trans. 2* **1987**, S1–S19.
- (29) Lucovsky, G.; Mooradian, A.; Taylor, W.; Wright, G. B.; Keezer, R. C. Identification of the Fundamental Vibrational Modes Of Trigonal, Monoclinic and Amorphous Selenium. *Solid State Commun.* **1967**, *5*, 113–117.
- (30) Alparone, A. Density Functional Theory Raman Spectra of Cyclic Selenium Clusters Se<sub>n</sub> (n=5-12). *Comput. Theor. Chem.* **2012**, *988*, 81–85.
- (31) Eysel, H. H.; Sunder, S. Homonuclear Bonds in Sulfur-Selenium Mixed Crystals: A Raman Spectroscopic Study. *Inorg. Chem.* **1979**, *18* (9), 2626–2627.
- (32) Kostyukevich, Y.; Kononikhin, A.; Popov, I.; Spasskiy, A.; Nikolaev, E. In ESI-Source H/D Exchange under Atmospheric Pressure for Peptides

- and Proteins of Different Molecular Weights from 1 to 66kDa: The Role of the Temperature of the Desolvating Capillary on H/D Exchange. *J. Mass Spectrom.* **2015**, *50* (1), 49–55.
- (33) Morgan, K. M.; Ashline, D. J.; Morgan, J. P.; Greenberg, A. Electrospray Ionization (ESI) Fragmentations and Dimethyldioxirane Reactivities of Three Diverse Lactams Having Full, Half, and Zero Resonance Energies. *J. Org. Chem.* **2014**, *79* (2), 517–528.
- (34) Li, J.; Chen, Z.; Wang, R.; Proserpio, D. M.; Strutturale, C.; Uni, I. Low Temperature Route towards New Materials: Solvothermal Synthesis of Metal Chalcogenides in Ethylenediamine. **1999**, *192*, 707–735.
- (35) Lu, J.; Xie, Y.; Xu, F.; Zhu, L. Study of the Dissolution Behavior of Selenium and Tellurium in Different Solvents—a Novel Route to Se, Te Tubular Bulk Single Crystals. *J. Mater. Chem.* **2002**, *12* (9), 2755–2761.
- (36) Tverjanovich, A.; Rodionov, K.; Bychkov, E. Raman Spectroscopy of Glasses in the As-Te System. *J. Solid State Chem.* **2012**, *190*, 271–276.
- (37) Brodsky, M. H.; Gambino, R. J.; Smith, J. E.; Yacoby, Y. The Raman Spectrum of Amorphous Tellurium. *Phys. Status Solidi* **1972**, *52* (2), 609–614.
- (38) Clark, E. R.; Collett, A. J. Preparation, Infrared and Raman Spectra of Some Compounds of Tellurium (II). *J. Chem. Soc. A Inorganic, Phys. Theor.* **1969**, 2129–2130.
- (39) Hendra, P. J.; Jovic, Z. Infrared and Raman Spectra of Some Complexes between Thiourea and Telluriun (II). *J. Chem. Soc. A Inorganic, Phys. Theor.* **1967**, 735–736.
- (40) Benamar, A.; Rayane, D.; Melinon, P.; Tribollet, B.; Broyer, M. Comparison between Selenium and Tellurium Clusters. *Zeitschrift für Phys. D Atoms, Mol. Clust.* **1991**, *19* (4), 237–239.
- (41) Mendoza-Galván, A.; García-García, E.; Vorobiev, Y. V.; González-Hernández, J. Structural, Optical and Electrical Characterization of Amorphous Se<sub>x</sub>Te<sub>1-x</sub> Thin Film Alloys. *Microelectron. Eng.* 2000, 51, 677–687.
- (42) Tverjanovich, A.; Cuisset, A.; Fontanari, D.; Bychkov, E. Structure of Se–Te Glasses by Raman Spectroscopy and DFT Modeling. *J. Am. Ceram. Soc.* **2018**, *101* (11), 5188–5197.

# **Supporting Information**

# Analyzing and Tuning the Chalcogen-Amine-Thiol Complexes for Tailoring of Chalcogenide Syntheses

Swapnil D. Deshmukh,<sup>†</sup> Leah F. Easterling,<sup>‡</sup> Jeremy M. Manheim,<sup>‡</sup> Nicole J. LiBretto,<sup>†</sup> Kyle G. Weideman,<sup>†</sup> Jeffrey T. Miller, <sup>†</sup> Hilkka I. Kenttämaa,<sup>‡</sup> and Rakesh Agrawal<sup>†</sup>\*

<sup>†</sup>Davidson School of Chemical Engineering, Purdue University, 480 Stadium Mall Drive, West Lafayette, IN 47907, United States <sup>‡</sup>Department of Chemistry, Purdue University, 560 Oval Drive, West Lafayette, Indiana 47907, United States

# **Selenium Dissolution in Monoamine vs Diamine Solutions:**

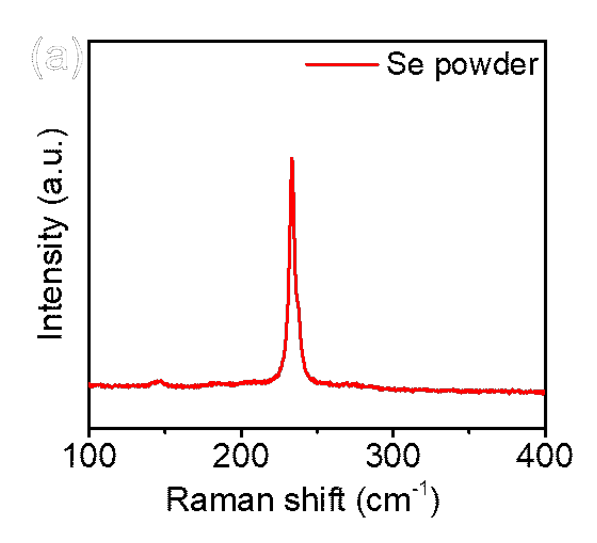


Figure S1: Raman spectra of metallic Se powder used for all the solution preparation

Table S1: Selected Raman band assignments for different Se structures

Structure	Raman frequency (cm <sup>-1</sup> )	Assignment
Trigonal	233	E
	237	A1
	273	2E
Orthorhombic	239	E3
	249	A1
	254	E2
Amorphous	235	Polymeric chain (A1, E)
	250	Se <sub>8</sub> (A1, E2)
Cyclic	279	Se <sub>5</sub> (A1)
	247	Se <sub>6</sub> (A1)
	285	Se <sub>7</sub> (A1)
	249	Se <sub>8</sub> (A1)
	264	Se <sub>9</sub> (A1)
	266	Se <sub>10</sub> (A1)
	258	Se <sub>12</sub> (A1)

## NMR analysis of Se-BA-ET and Se-EN-ET solutions:

<sup>1</sup>H-NMR spectra were collected on a Brucker AV-III-400-HD instrument at 400 MHz frequency using CD<sub>3</sub>CN as the solvent. Since the addition of amines to thiols lead to proton transfer reactions, the actual species present in solution are alkyl ammonium ions and thiolate ions. The byproduct of Se dissolution, dialkyl disulfides, were also confirmed from NMR analysis. Structures of all proton containing species are shown below with each distinct proton labeled separately. These labeles are then used to assign corresponding peaks in <sup>1</sup>H-NMR spectra.

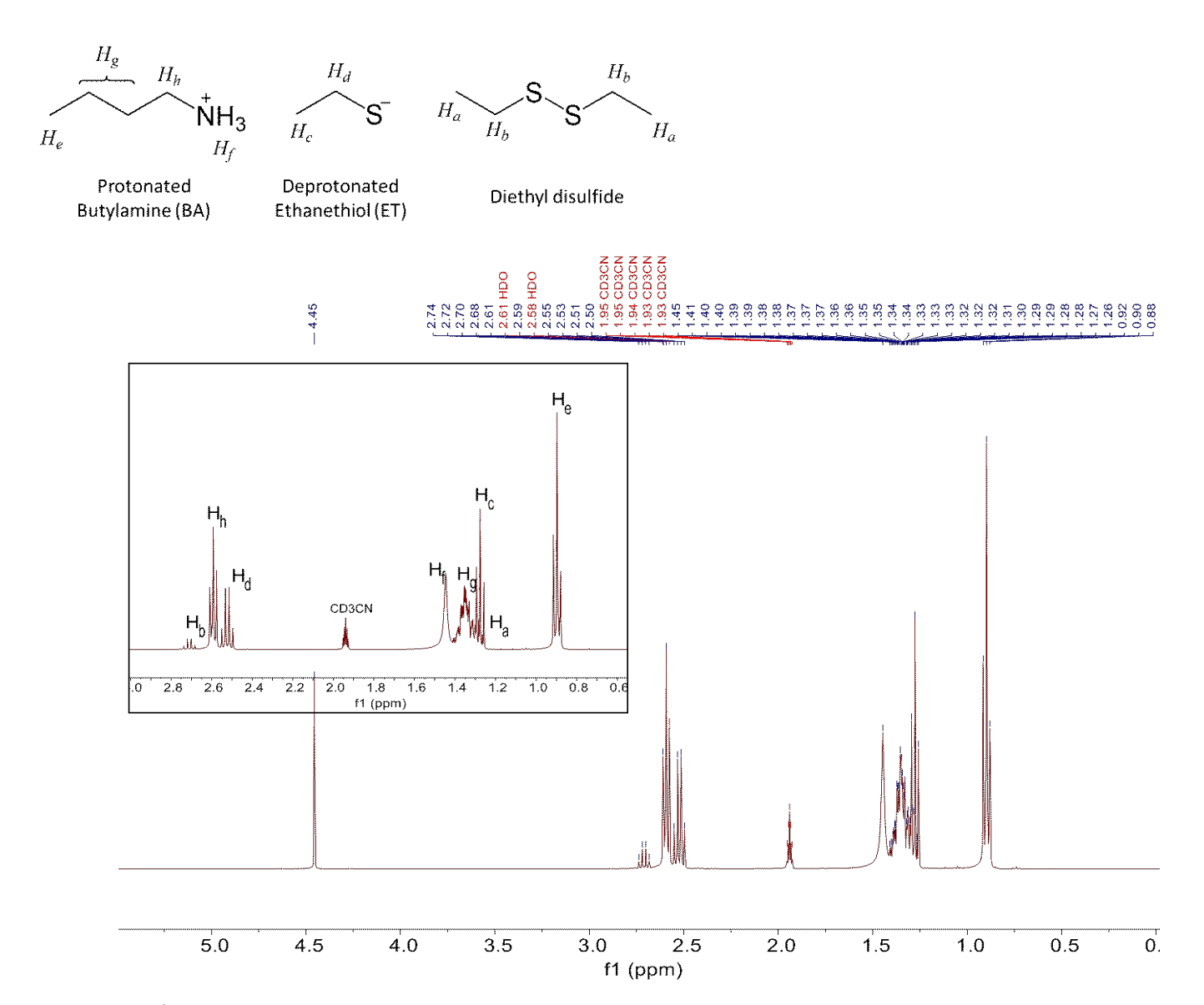
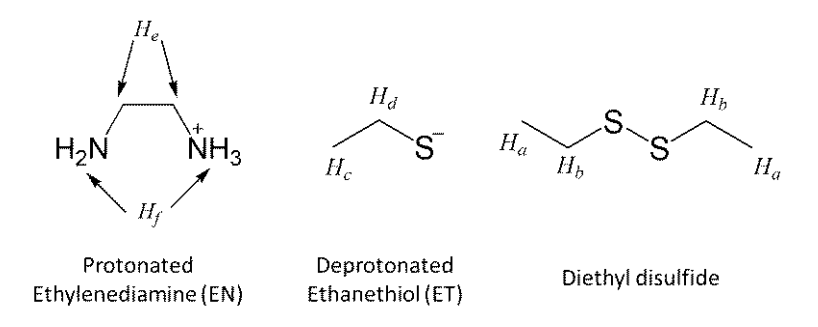


Figure S2:  $^{1}$ H-NMR of Se-BA-ET solution with protons labeled according to strcures presented above. (Peak at  $\delta$  of 4.45 ppm corresponds the ethylene carbonate used as NMR standard)



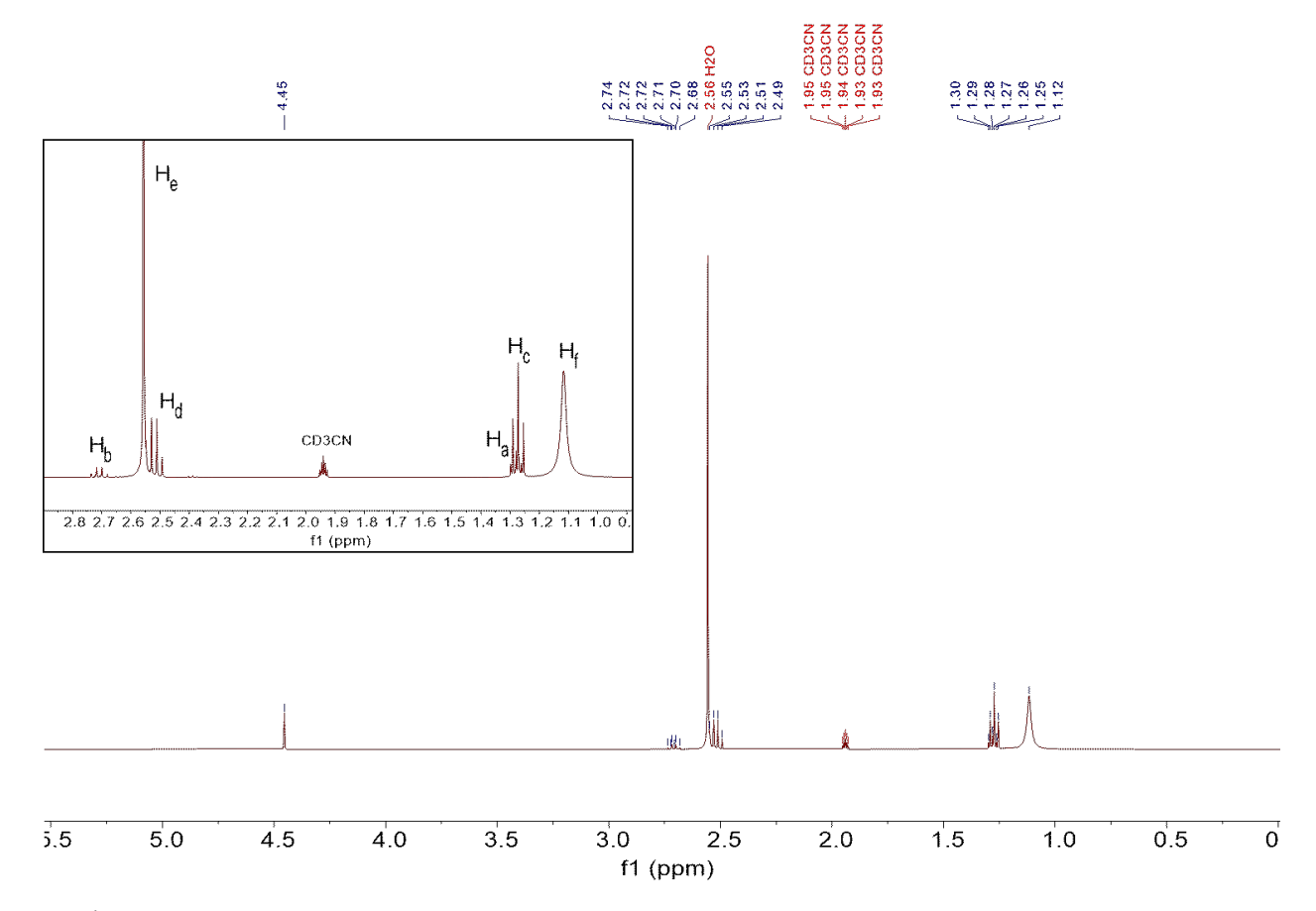


Figure S3:  $^{1}$ H-NMR of Se-EN-ET solution with protons labeled according to strcures presented above. (Peak at  $\delta$  of 4.45 ppm corresponds the ethylene carbonate used as NMR standard)

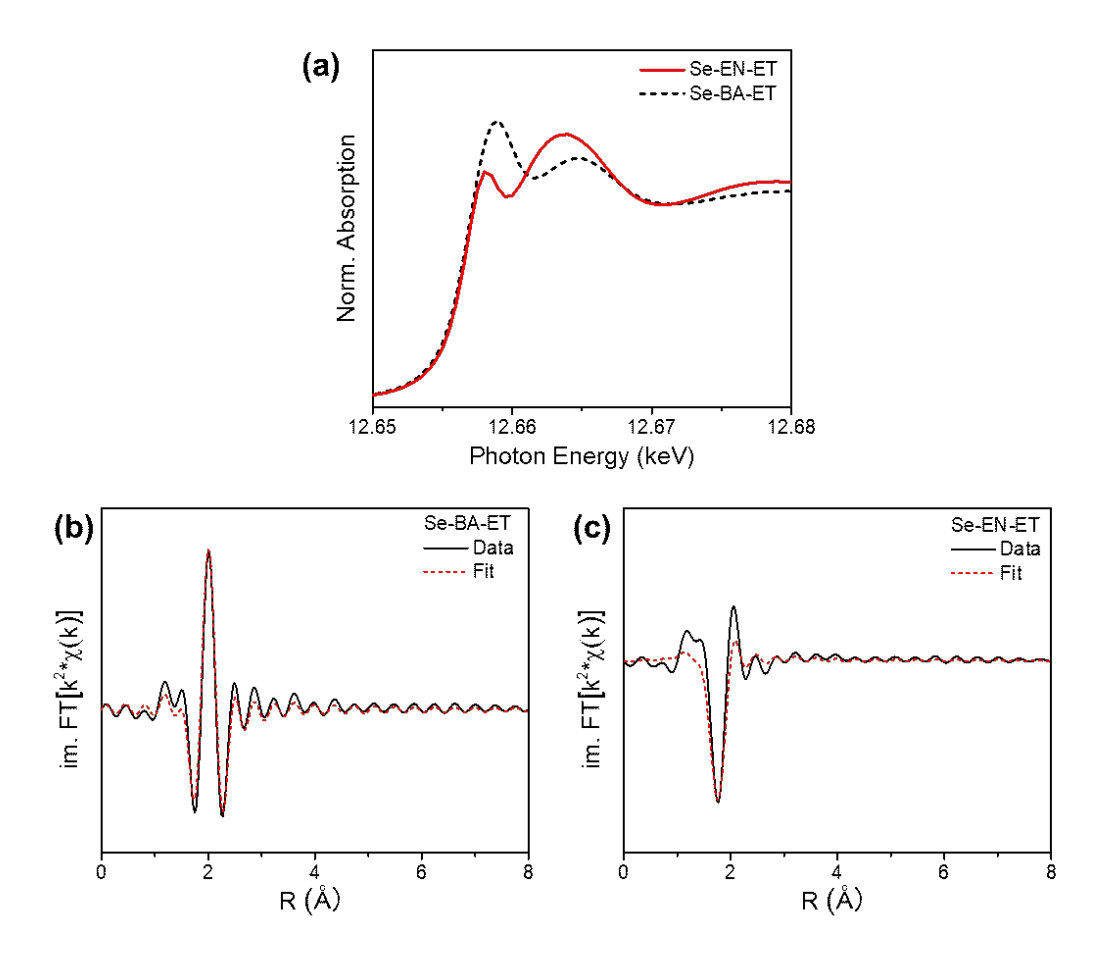


Figure S4: (a) the K-edge XANES spectra and (b,c) the imaginary component of the Fourier transforms (FTs) of Se K-edge k2-weighted EXAFS spectra for Se dissolved in BA-ET and EN-ET solutions with 1:1 (v/v) amine:thiol used for dissolution

### (-) ESI-MS analysis of Se-BA-ET and Se-EN-ET solutions:

Ions observed and identified in (-) ESI-MS high-resolution mass spectra of Se-BA-ET and Se-EN-ET solutions are summarized in Table 1. The m/z values listed correspond to the monoisotopic mass for each ion. Elemental compositions and the associated error with respect to the observed m/z vales are also given for each ion. For some ions, the high resolution MS signal was too low for accurate calculation of the error or calculation of the m/z with high accuracy (more than two decimal points). Assignments for these ions were based on low-resolution mass spectra and isotopic distributions. These ions are marked with \*.

Table S2: Elemental composition of ions detected using (-) ESI-MS for Se solutions in BA-ET and EN-ET

Se in BA-ET			
m/z	<b>Elemental Composition</b>	Error from expected mass (+/- ppm)	
112.89743	HSSe	13.83	
148.02660	$C_5H_{10}NS_2$	11.03	
160.84253	$HSe_2$	13.71	
227.94314	$C_5H_{10}NS_2Se$	10.41	
240.75861	HSe <sub>3</sub>	7.34	
320.67581	HSe <sub>4</sub>	7.63	
400.59277	HSe <sub>5</sub>	5.68	
474.00*	HSe <sub>6</sub>	Signal too low, assigned based on isotopic patterns	
550.50*	HSe <sub>7</sub>	Signal too low, assigned based on isotopic patters	

Se in EN-ET		
m/z	<b>Elemental Composition</b>	Error from expected mass (+/- ppm)
80.92523	HSe	17.69
92.98412	$C_2H_5S_2$	15.08
111.88941	SSe	12.21
140.92852	$C_2H_5SSe$	9.58
160.84194	$HSe_2$	10.07

# **Effect of Thiol Quantity on Selenium Dissolutions:**

### Raman analysis of Se-BA-ET solutions at different concnetrations:

Figure S5a compiles the Raman spectra for samples with fixed thiol:Se ratio (ET:Se=0.3) at different Se concentrations. These spectra suggest that with amine dilution, the relative ratio of amine peak intensity to Se-Se peak intensity increases. However, all samples show two identical peaks corresponding to polyselenides (linear and possibly cyclic) suggesting no significant effect of Se concentration on the species formed in the solution with amine dilution within 0.01 M - 1.25 M concentration range and fixed thiol:Se ratio. Similarly, Figure S5b compiles the Raman spectra for samples with fixed amine:thiol ratio (BA:ET=5) at different Se concentrations. These solutions yield thiol:Se ratio of 1.5, 12 and 120 for 1.25 M, 0.1 M and 0.01 M samples respectively. As can be seen from the Raman spectra below, this dilution with amine-thiol solution results in drastic increase in intensity for amine and thiol peaks making the relative intensity of Se-Se peak smaller. When analyzed closely, these spectra show presence of a peak at around 246 cm<sup>-1</sup>. Although the peak positions look similar, the peak for higher concentration samples appear skewed with small shoulder on the lower frequency side while the peak for 0.01 M sample looks symmetric. Such non skewed peak for 0.01 M sample could be a result of either steeply decreasing baseline in this sample at lower frequencies hiding this shoulder (mostly arising from strong solvent scattering) or reduced distribution of polyselenides in the solution. While other experiments might be needed to deconvolute this observation, it is important to note that even with extreme dilution using amine-thiol solution (0.01 M Se concentration and thiol:Se ratio of 120) the Se species remain in the form of polyselenides.

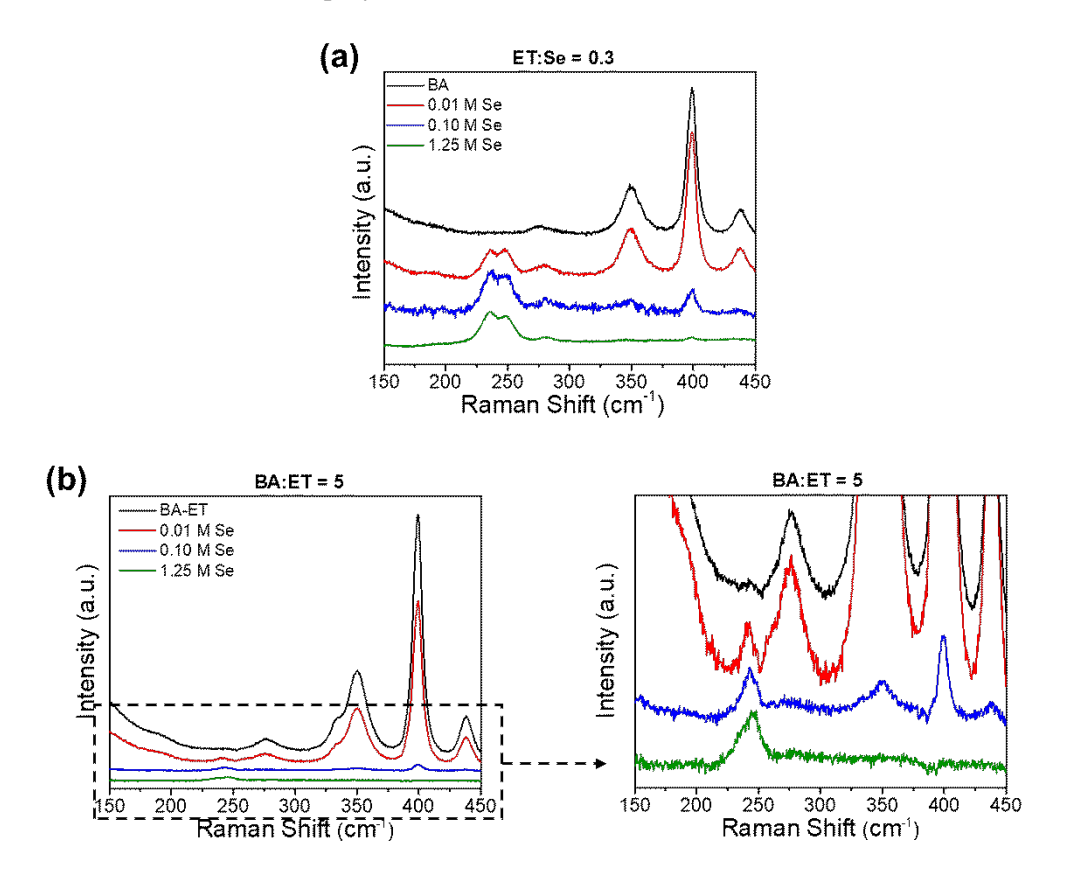


Figure S5: Raman spectra of Se-BA-ET solution collected at different concentrations by keeping (a) ET:Se fixed at 0.3 and (b) BA:ET fixed at 5

# X-ray Absorption Spectroscopy of Se-BA-ET and Se-EN-ET solutions with minimmum ET:

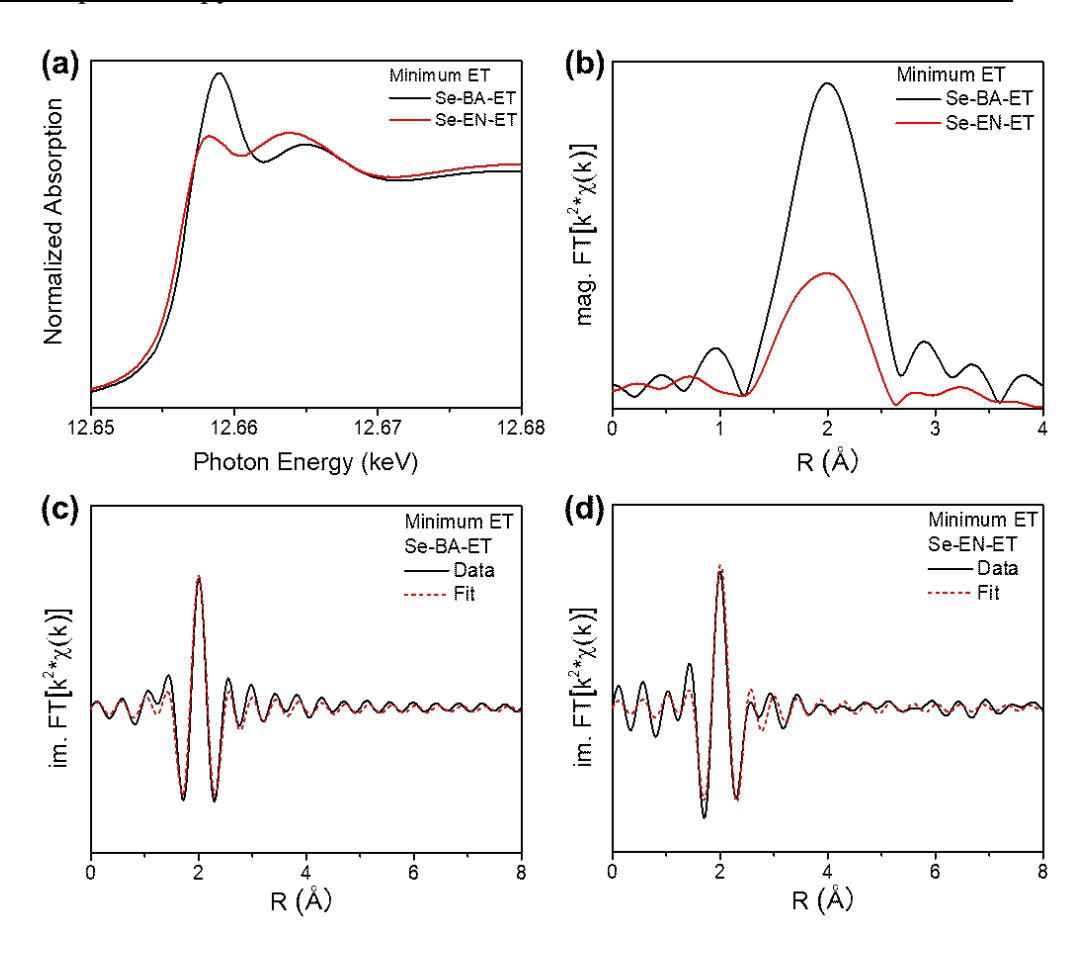


Figure S6: (a) Se K-edge XANES spectra, (b) the magnitude component and (c.d) the imaginary component of the Fourier transforms (FTs) of Se K-edge k2-weighted EXAFS spectra measured for Se in BA-ET and Se in EN-ET solutions with minimum ET used for dissolution

## NMR analysis of Se-BA-ET solutions with different thiol quantities:

<sup>1</sup>H-NMR spectra were collected on a Brucker AV-III-400-HD instrument at 400 MHz frequency using CD<sub>3</sub>CN solvent. Ethylene carbonate was used as NMR standard for quantitative analysis. Additional ET in Se-BA solution leads to the formation of diethyldisulfide and its quantity was calculated by integrating the quartet peak at δ of 2.72 ppm.

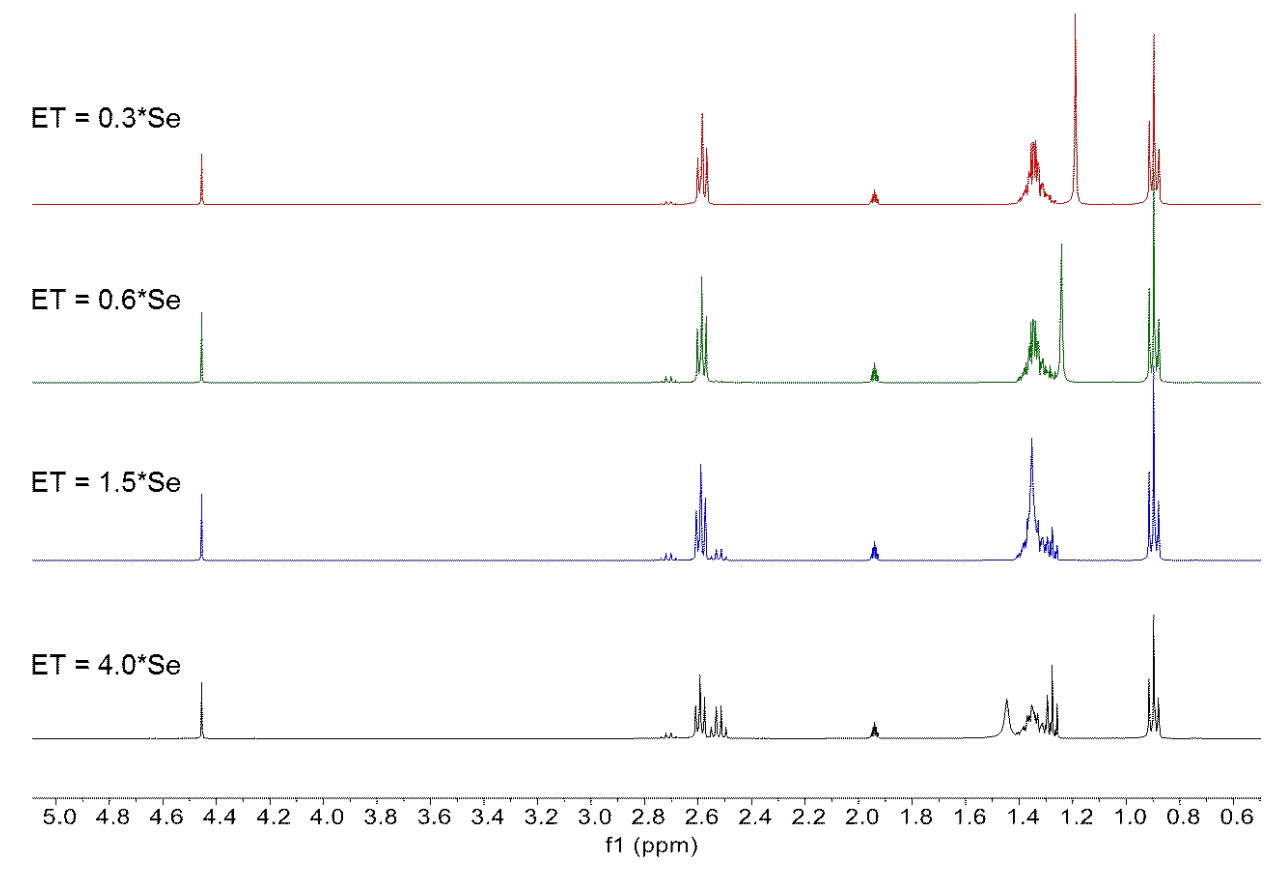


Figure S7:  $^{1}$ H-NMR speactra of Se-BA-ET solutions with different quantity of thiol used for dissolution. Quartet at  $\delta$  of 2.72 ppm corresponding to diethyldisulfide was used for quantitative measurement with reference to the peak at  $\delta$  of 4.45 ppm corresponding the ethylene carbonate as NMR standard.

## (-) ESI-MS analysis of Se-BA-ET and Se-EN-ET solutions with minimum ET:

(-) ESI-MS spectra of Se-BA-ET and Se-EN-ET solutions containing minimum ET quantity are shown in Figure S8. Ions observed and identified in these spectra along with their proposed chemical composition are summarized in Table 2. The m/z listed corresponds to the monoisotopic mass for the ion.

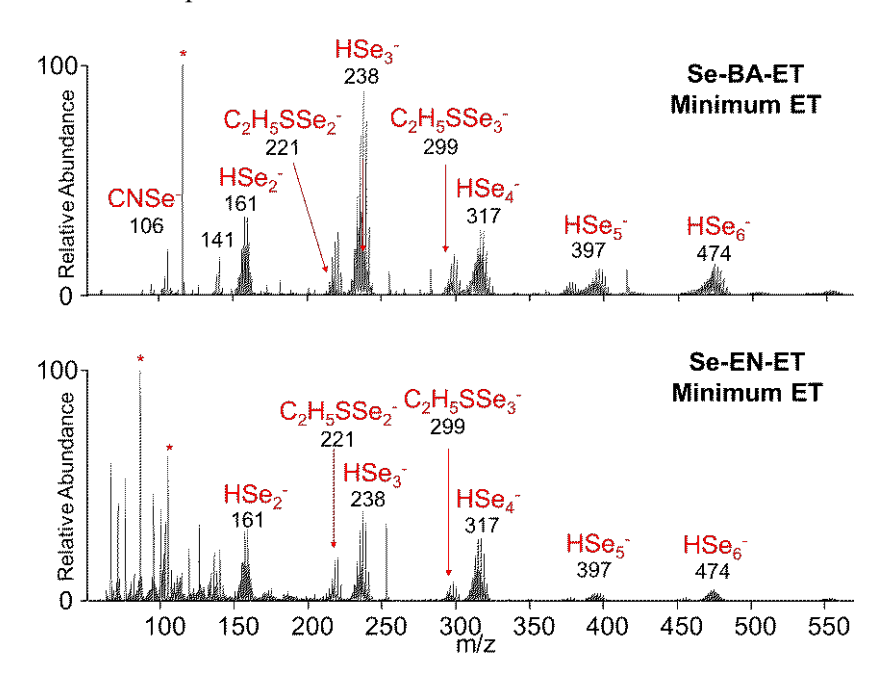


Figure S8: (-) ESI-MS spectra of Se-BA-ET solution and Se-EN-ET solution with minimum thiol used for dissolution

For some ions, the high resolution MS signal was too low for accurate calculation of the error or calculation of the m/z with high accuracy (more than two decimal points). Assignments for these ions were based on low-resolution mass and isotopic distributions. These ions are marked in the table with \*.

Table S3: Elemental composition of ions detected using (-) ESI-MS for Se solutions in BA-ET and EN-ET with minimum thiol used for dissolution

Se in BA-ET with minimum ET		
m/z	<b>Elemental Composition</b>	Error from expected mass (+/- ppm)
105.92037	CNSe	11.73
116.07191	$C_5H_{10}NO_2$	11.24
140.92850	$C_2H_5SSe$	9.59
159.83391	$\mathrm{Se}_2$	8.98
220.84506	$C_2H_5SSe_2$	6.20
240.75812	$HSe_3$	6.69
300.76171	$C_2H_5SSe_3$	5.14
320.67536	HSe <sub>4</sub>	5.66
400.59350	HSe <sub>5</sub>	8.35
480.58*	HSe <sub>6</sub>	Signal too low

Se in EN-ET with minimum ET		
m/z	<b>Elemental Composition</b>	Error from expected mass (+/- ppm)
85.047079	C <sub>3</sub> H <sub>5</sub> ON <sub>2</sub>	13.53
108.99644	$C_2H_5O_3S$	9.62
140.92818	$C_2H_5SSe$	7.17
160.84161	$HSe_2$	8.02
220.84452	$C_2H_5SSe_2$	3.75
240.75800	HSe <sub>3</sub>	4.81
300.76146	$C_2H_5SSe_3$	4.15
319.66712	Se <sub>4</sub> /HSe <sub>4</sub>	4.95
400.59241	HSe <sub>5</sub>	6.30
480.58*	HSe <sub>6</sub>	Signal too low

## NMR analysis of Se-EN-ET solutions with different thiol quantities:

 $^{1}$ H-NMR spectra were collected on a Brucker AV-III-400-HD instrument at 400 MHz frequency using CD<sub>3</sub>CN solvent. Ethylene carbonate was used as NMR standard for quantitative analysis. Additional ET in Se-BA solution leads to the formation of diethyldisulfide and its quantity was calculated by integrating the quartet peak at δ of 2.72 ppm.

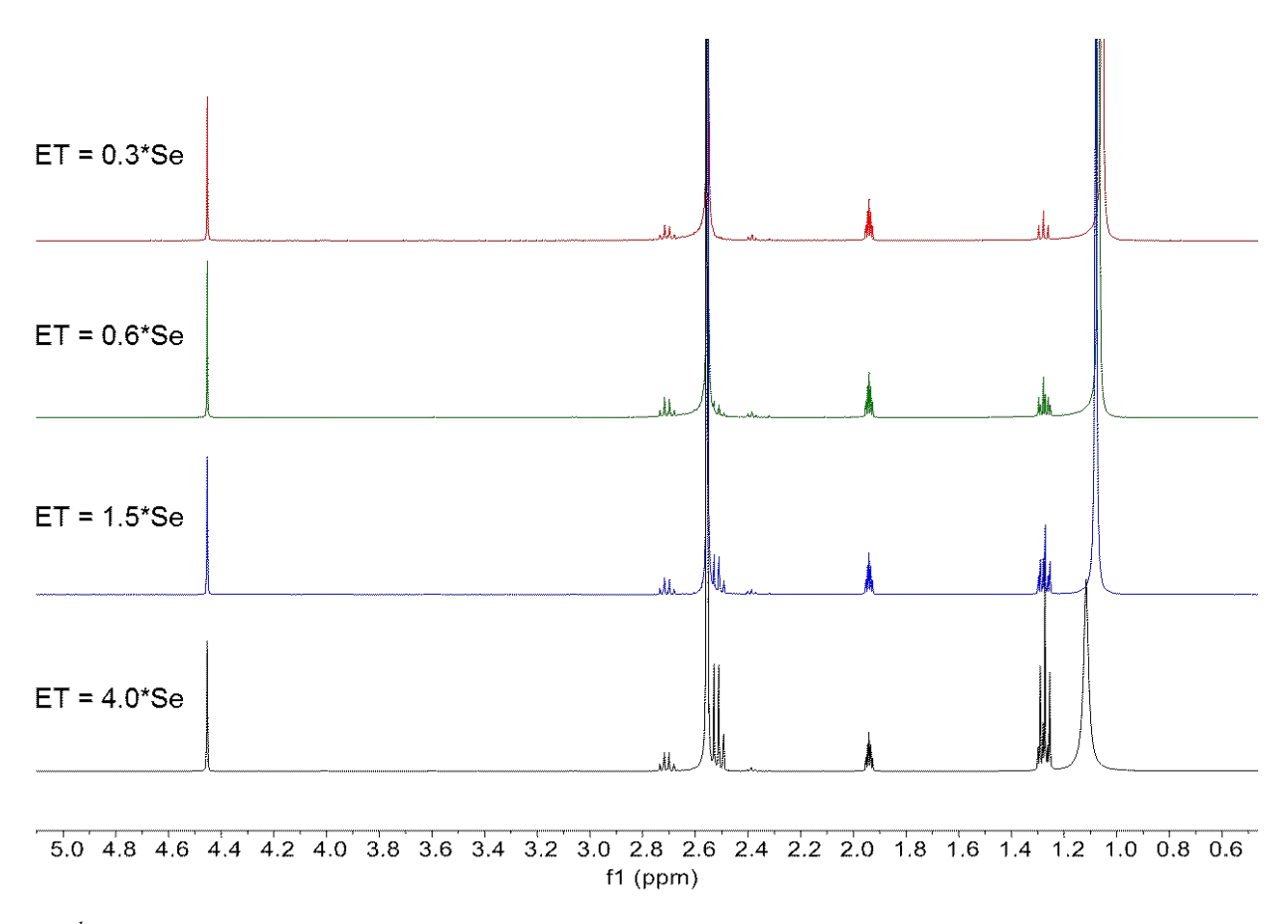


Figure S9:  $^{1}$ H-NMR speactra of Se-EN-ET solutions with different quantity of thiol used for dissolution. Quartet at  $\delta$  of 2.72 ppm corresponding to diethyldisulfide was used for quantitative measurement with reference to the peak at  $\delta$  of 4.45 ppm corresponding the ethylene carbonate as NMR standard.

# **Tellurium Dissolution in Diamine Solutions:**

# X-ray Absorption Spectroscopy of Te-EN-ET solution:

Figure S10 summarizes XAS analysis of Te in EN-ET solution.

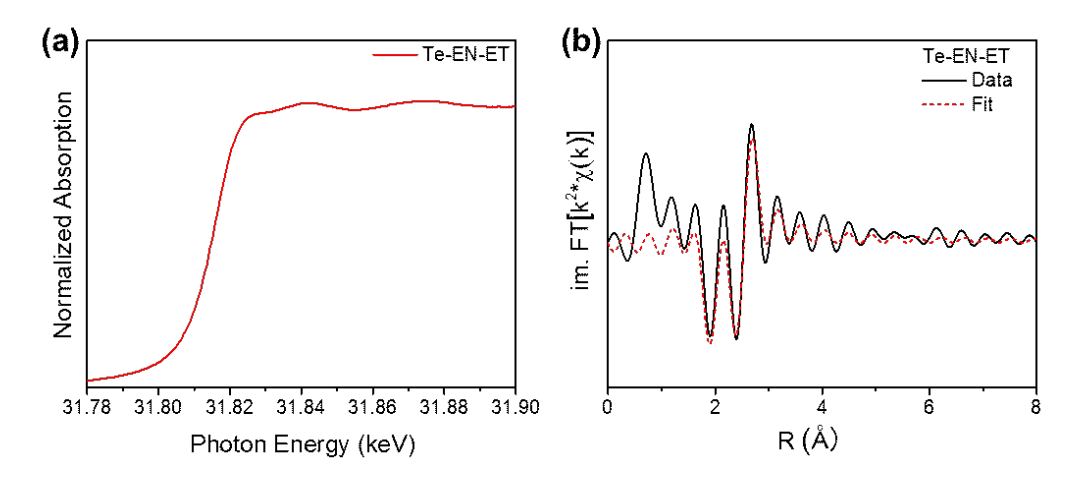


Figure S10: (a) Te K-edge XANES spectra, (b) the imaginary component of the Fourier transforms (FTs) of Te K-edge k2-weighted EXAFS spectra measured for Te in EN-ET solution

## (-) ESI-MS analysis of Te-EN-ET solution:

Ions observed and identified in (-) ESI-MS spectra of Te-EN-ET solution are summarized in Table 3. The m/z listed corresponds to the monoisotopic mass for each ion. Elemental compositions and the corresponding error with respect to the observed m/z are also calculated for each ion. For some ions, the high resolution MS signal was too low for accurate calculation of the error or calculation of the m/z with high accuracy (more than two decimal points). Assignments for these ions were based on low-resolution mass and isotopic distributions. These ions are marked in the table with \*.

Table S4: Elemental composition of ions detected using (-) ESI-MS for Te solutions in EN-ET

Te in EN-ET		
m/z	<b>Elemental Composition</b>	Error from expected mass (+/- ppm)
136.95613	$C_3H_5S_3$	9.79
161.87906	STe	8.12
190.91805	$C_2H_5STe$	6.19
260.82089	$HTe_2$	4.48
320.82420	$C_2H_5STe_2$	3.45
389.71815	Te <sub>3</sub> /HTe <sub>3</sub>	0.08
450.75*	C <sub>2</sub> H <sub>5</sub> STe <sub>3</sub>	Signal too low
520.67*	$HTe_4$	Signal too low

# Co-dissolution of Tellurium and Selenium:

## X-ray Absorption Spectroscopy of Se-Te-BA-ET and Se-Te-EN-ET solutions:

Figure S11 summarizes XAS analysis of Se-Te co-dissolution in BA-ET and EN-ET solutions. The XANES spectra for these two solutions look very similar but the EXAFS analysis of the collected data suggests some difference between neighboring environments of the Se in these two solutions.

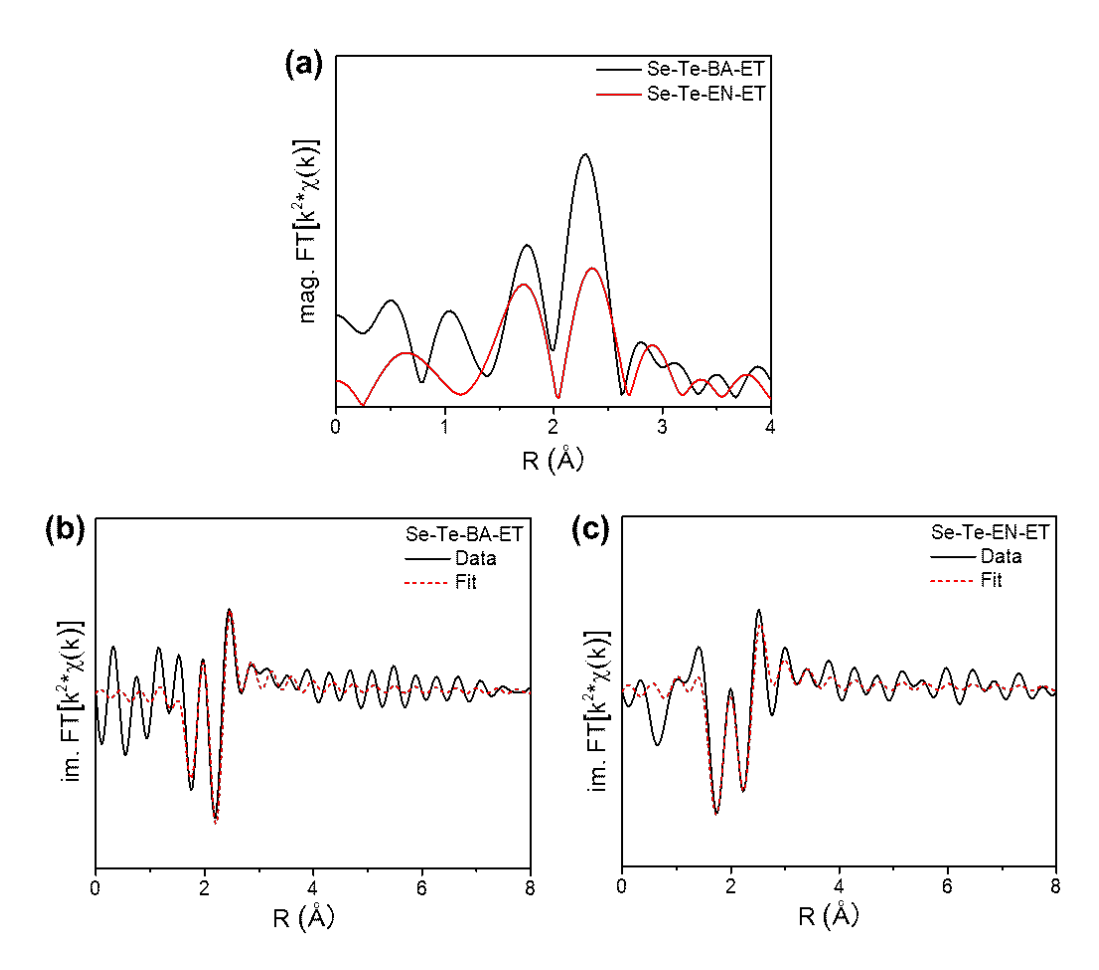


Figure S11: (a) The magnitude component and (c,d) the imaginary component of the Fourier transforms (FTs) of Se K-edge k2-weighted EXAFS spectra of Se-Te-BA-ET and Se-Te-EN-ET solutions.

### (-) ESI-MS analysis of Se-Te-BA-ET and Se-Te-EN-ET solutions:

Ions observed and identified in (-) ESI-MS spectra of Se-Te-BA-ET and Se-Te-EN-ET solutions are summarized in Table 4. The m/z listed corresponds to the monoisotopic mass for each ion. Elemental compositions and the associated error with respect to observed m/z are also calculated for each ion. For some ions, the high resolution MS signal was too low for accurate calculation of the error or calculation of the m/z with high accuracy (more than two decimal points). Assignments for these ions were based on low-resolution mass and isotopic distributions. These ions are marked in the table with \*.

Table S5: Elemental composition of ions detected using (-) ESI-MS for Se-Te solutions in BA-ET and EN-ET

Se-Te in BA-ET		
m/z	<b>Elemental Composition</b>	Error from expected mass (+/- ppm)
105.92036	CNSe	12.39
148.02625	$C_5H_{10}NS_2$	9.00
160.84213	$HSe_2$	11.25
210.83132	HSeTe	6.16
227.94271	$C_5H_{10}NS_2Se$	5.58
289.73993	Se <sub>2</sub> Te	4.18
370.66490	HSe₃Te	4.95
420.83*	$HSe_2Te_2$	Signal too low
500.67*	HSe <sub>3</sub> Te <sub>2</sub>	Signal too low

Se-Te in EN-ET		
m/z	<b>Elemental Composition</b>	Error from expected mass (+/- ppm)
105.91988	CNSe	7.86
140.92789	$C_2H_5SSe$	5.11
155.90941	CNTe	4.24
160.84100	$HSe_2$	4.23
190.91736	C <sub>2</sub> H <sub>5</sub> STe	2.56
212.84688	H <sub>3</sub> SeTe	5.68
259.81210	$Te_2$	0.78
270.83359	$C_2H_5SSeTe$	0.73
289.73917	$Se_2Te$	1.56
320.82318	$C_2H_5STe_2$	0.27
340.83*	$HSeTe_2$	Signal too low
370.75*	HSe₃Te	Signal too low
420.83*	$HSe_2Te_2$	Signal too low

# **Tuning Material Synthesis through Discovered Chemical Understanding:**

 $\underline{SEM} \ analysis \ of \ PbSe_nTe_{1-n} \ particles \ synthesized \ from \ Se-Te-BA-ET \ and \ Se-Te-EN-ET \ solutions:$ 

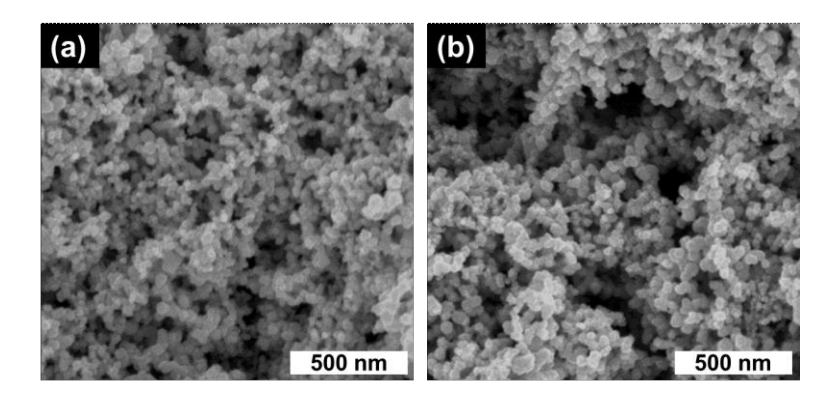


Figure S12: SEM images of the  $PbSe_nTe_{1-n}$  particles synthesized using (a) Se-Te-BA-ET solution and (b) Se-Te-EN-ET solution